



UNIVERSITÀ DEGLI STUDI DI VERONA

Department of Diagnostics and Public Health

*PhD Course in Nanoscience and Advanced Technology –
Technologies and nanotechnology in forensic sciences*

XXXVI Cycle (2020-2023)

ZEBRAFISH LARVAE AS AN ALTERNATIVE ANIMAL MODEL TO STUDY TOXICITY OF NEW SYNTHETIC OPIOIDS

S.S.D. MED/43




Coordinator: Prof. Adolfo Speghini

Tutor: Prof. Rossella Gottardo

PhD Student: Matilde Murari

This work is licensed under a Creative Commons Attribution-NonCommercial-NoDerivs 3.0 Unported License, Italy. To read a copy of the licence, visit the web page:

<http://creativecommons.org/licenses/by-nc-nd/3.0/>

-  **Attribution** — You must give appropriate credit, provide a link to the license, and indicate if changes were made. You may do so in any reasonable manner, but not in any way that suggests the licensor endorses you or your use.
-  **NonCommercial** — You may not use the material for commercial purposes.
-  **NoDerivatives** — If you remix, transform, or build upon the material, you may not distribute the modified material.

Zebrafish larvae as an alternative animal model to study toxicity of new synthetic opioids

Matilde Murari

PhD thesis

Place and date of submission to U-GOV University Research Catalogue

ISBN Code

*«Omnia venenum sunt:
nec sine veneno quicquam existit.
Dosis sola facit, ut venenum non fit.»*

Paracelso

ABBREVIATIONS

AO	Acridine Orange
APCI	Atmospheric Pressure Chemical Ionization
CYP	Cytochrome P
DOR	Delta-Opioid Receptor
dpf	days post fertilization
EMCDDA	European Monitoring Centre for Drugs and Drug Addiction
ESI	ElectroSpray Ionization
EWA	Early Warning Advisor
EWS	Early Warning System
FuF	2-FuranylFentanyl
FT-ICR	Fourier transform ion cyclotron resonance
FW	Fish Water
GTP	Guanosine TriPhosphate
hpf	hours post fertilization
HRAM	High Resolution Accurate Mass
HRMA	High Resolution Mass Analyzer
HRMS	High Resolution Mass Spectrometry
J	Jaw
KOR	Kappa-Opioid Receptor
LC	Liquid Chromatography
m/z	mass to charge ratio
MOR	Mu-Opioid Receptor
MS	Mass Spectrometry
MTC	Maximum Tolerated Concentration
NPS	New Psychoactive Substances
NSO	New Synthetic Opioids
OcF	Ocfentanyl
PE	Pericardial Edema
ppm	parts per millions
PTU	PhenylThioUrea

QqQ	Triple Quadrupole
QTOF	Quadrupole-Time Of Flight
R	Resolution
ReTOF	Reflectron Time Of Flight
RF	Radio Frequency
ROI	Region Of Interest
RP	Reverse Phase
LC-MS	Liquid Chromatography-Mass Spectrometry
RT	Retention Time
SC	Spinal Curvature
SULT	Sulfotransferase
THC	TetraHydroCannabinol
TIC	Total Ion Chromatogram
TOF	Time Of Flight
UGT	UDP-glucuronosyltransferase
UNODC	United Nations Office on Drugs and Crime
YSE	Yolk Sac Edema
ZL	Zebrafish Larvae

ABSTRACT

In forensic toxicology, a problem of global concern is represented by the continuous rapid emergence of New Psychoactive Substances (NPS) due to several factors, including multiplicity of chemical structures, poorly known activity, short half-life in the illicit drug market, and lack of pure standards. Among these problems, the lack of information about metabolism and adverse effects is also of the highest relevance.

Nowadays, opioids and, in particular, synthetic opioids are of high concern since they represent one of the fastest-growing groups of NPS. For this reason, a new rapid screening tool is needed to keep up with the timing of releasing these new compounds in the drug market.

In the present thesis work, zebrafish larvae have been tested as an alternative animal model with the effort to study the NPS, exploiting the advantages that this model offers compared to other *in vivo* studies (i.e., high reproducibility, low cost, and less ethical issues).

To this aim, the first step of this study was dedicated to developing a new protocol for evaluating the toxicity of new synthetic opioids. Thus, zebrafish larvae have been exposed to a relatively known opioid (i.e., fentanyl) to test the validity of the zebrafish larvae (ZL) model, which had been rarely used in forensic toxicology so far. The investigation involved behavioral and metabolic assay and morphological defect evaluation. In parallel, the mice model was used for comparison.

To test behavioral effects, larvae were exposed to 1 and 10 μM concentrations on the fourth-day post-fertilization. The locomotor activity was evaluated as distance moved in the unit of time and registered with a tracking system. Using ZL, it was possible to highlight the presence of several morphological abnormalities when exposed to high fentanyl doses (50, 100 μM).

For the metabolic assay, a 1260 Infinity LC coupled to a 6540 Accurate-Mass QTOF spectrometer was used for identification of metabolites after exposing ZL for 24 hours to fentanyl (1 and 10 μM).

In a second step, ocfentanil and 2-furanylfentanyl were selected as target compounds. These drugs belong to the class of synthetic opioids, but only a few

data were available in the literature regarding their toxicity and remarkably, no data about their metabolic fate. The same behavioral and metabolic assay protocols were applied, and data were compared with those obtained in mice. Overall, the obtained results confirm the validity of ZL for identifying metabolites, and only minor differences in metabolism were observed when compared to mice.

The last part of the thesis project was focused on the metabolic assay, and on the analysis of a panel of n=9 New Synthetic Opioids (NSO), namely, AP-237 and 2-methyl-AP-237, isotonitazene, flunitazene, etodesnitazene, metonitazene, metodesnitazene, N-pyrrolidino etonitazene, and butonitazene. On the fourth day post-fertilization, larvae were exposed for 24 hours to 1 μM concentration and analyzed with a Vanquish UPLC coupled with an Orbitrap Fusion™ Lumos™ Tribrid™ Mass Spectrometer. Moreover, an *in vivo* cell death assay was performed to test and quantify the toxicity level of these compounds: the acridine orange was applied after 24h exposure to 0.1 μM of each drug. The number of fluorescent dots (corresponding to a cluster of apoptotic cells) was quantified: all the tested compounds exhibited a toxicity level significantly higher than the control.

The results of this thesis project, clearly support the suitability of the zebrafish larvae model as an effective platform to rapidly assess synthetic opioid toxicity.

TABLE OF CONTENTS

ABBREVIATIONS.....	4
ABSTRACT.....	6
TABLE OF CONTENTS	8
1. NEW PSYCHOACTIVE SUBSTANCES	10
1.2 New Synthetic Opioids (NSO).....	11
1.2.1 The emerging problem of NSO	13
2. ANIMAL MODELS	14
2.1 Zebrafish	14
2.1.1 Morphological assay in zebrafish.....	17
2.1.2 Metabolic studies in zebrafish.....	17
2.1.3 Behavioral assays in zebrafish.....	18
3. ANALYTICAL TECHNIQUES.....	20
3.1 Liquid Chromatography coupled with mass spectrometry (LC-MS)	20
3.1.1 Ionization sources.....	23
3.1.1.1 The Electro Spray Ionization (ESI) technique.....	24
3.1.2 Mass Analyzer.....	24
3.1.2.1 Quadrupole analyzer.....	26
3.1.2.2 Time of Flight (TOF) analyzer.....	27
3.1.2.3 Orbitrap analyzer.....	28
3.1.3 Detector	29
3.1.4 Acquisition modes	30
3.1.4.1 Full scan mode.....	30
3.1.4.2 Target MS/MS.....	31
3.2 DanioVision tracking system	31
4. AIMS OF THE THESIS PROJECT.....	33
5. EXPERIMENTAL PART.....	35
5.1 Animal Husbandry and Ethic Statement.....	35
5.2 ZL applied in the study of behavioral effects and metabolism of fentanyl.....	37
5.2.1 Fentanyl.....	37
5.2.2 Materials and Methods	38
5.2.2.1 Maximum-tolerated concentrations assay	38
5.2.2.2 Behavioral assay.....	39
5.2.2.3 Metabolic assay.....	40
5.2.2.4 Statistical analysis.....	41
5.2.3 Results	42
5.2.3.1 Maximum-tolerated concentrations assay	42
5.2.3.2 Behavioral assay.....	43

5.2.3.3 Metabolic assay	45
5.2.4 Discussion.....	48
5.3 Study of toxicity and behavioral effects of ocfentanil and 2-furanylfentanyl in zebrafish larvae and mice.....	51
5.3.1 Ocfentanil and 2-furanylfentanyl.....	51
5.3.3 Materials and Methods	53
5.3.3.1 Morphological assay.....	53
5.3.3.1 Behavioral assay.....	53
5.3.3.3 Metabolic assay	54
5.3.3.4 Statistics.....	54
5.3.4 Results	55
5.3.4.1 Morphological assay.....	55
5.3.4.2 Behavioral assay.....	56
5.3.4.3 Metabolic assay	58
5.3.5 Discussion.....	63
5.4 Study of metabolism and potential toxicity of nine synthetic opioid analogs using the zebrafish larvae model	66
5.4.1 Cinnamylpiperazine.....	66
5.4.2 Benzylbenzimidazole.....	67
5.4.3 Materials and Methods	69
5.4.3.1 In vivo cell death assay.....	69
5.4.3.2 Morphological assay.....	69
5.4.3.3 Metabolic assay	70
5.4.4 Results	71
5.4.4.1 In vivo cell death assay.....	71
5.4.4.2 Morphological assay.....	73
5.4.4.3 Metabolic assay	73
5.4.5 Discussion.....	79
6. FINAL CONCLUSION	82
REFERENCES	86

1. NEW PSYCHOACTIVE SUBSTANCES

New Psychoactive Substances (NPS) have been defined by The United Nations Office for Drugs and Crime (UNODC) as “*substances of abuse, either in a pure form or a preparation, that are not controlled by the 1961 Single Convention on Narcotic Drugs or the 1971 Convention on Psychotropic Substances, but which may pose a public health threat*”¹. The term “new” does not necessarily refer to the synthesis of original chemical structure but sometimes to the new use as “legal highs”² of old molecules that have only recently become commercially available. The definition can vary between countries, reflecting differences in national legislations³, but also during time for the continuous effort to control the spread of these new drugs.

From the early to mid-2000s, NPS are reportedly present all over the world; this rapid emergence is also due to the continuous chemical modifications in the market to evade the legislation.

The two of the major organizations monitoring NPS - the UNODC and the European Monitoring Centre on Drugs and Drug Addiction [EMCDDA] - annually report the number and the type of NPS notified for the first time. This number reach a peak in 2014 of 101 new substances identified. According to their data, even if the total number of NPS identified increases each year, the number of new substances detected has declined since 2016^{4,5}. Nevertheless, their penetration increased in the market of prescribed medicine; the main problem with these substances is that they tend to be analogues of existing pharmaceutical drugs, with the aim of mimic the effect of licensed medicines³, but without real data regarding their potency and their pharmacological/toxicological properties. Moreover, NPS are sold as or mixed with more established illicit drugs, leading to unexpected effect in the short and in the long term or even overdoses².

According to the UNODC data, as October 2023, the number of NPS is 1230, reported in 141 different countries. Therefore, this group of substances is huge and heterogenous and even the classification is challenging and not always commonly

accepted. For the UNODC Early Warning Advisor (EWA), a possible subdivision is the effect group classification⁶. The main substance groups of NPS are:

1. Classic hallucinogens, comprehending phenethylamines, tryptamines and lysergamides; these compounds have stimulants effect, with a potent agonist or antagonist activity at various serotonin and dopamine receptors.
2. Synthetic opioids, representing fentanyl analogues and nitazenes; this class includes substances with analgesic effect originally developed as medicinal drugs.
3. Sedatives/hypnotics group including designer benzodiazepines.
4. Dissociatives, comprehending phencyclidine type substances and ketamines, with a dissociative effect in the central nervous system.
5. Stimulants, which is a huge group including synthetic cathinones, phenethylamines, aminoindanes, phenidates, piperazines and other substances.
6. Synthetic cannabinoids, this is a wide class of compounds, comprehending all the molecules chemically related to THC, but with higher potency.

Regarding their prevalence, until 2013 the majority of NPSs consisted of synthetic cannabinoids and synthetic cathinones⁷. These groups are still the most popular, but in recent years the synthetic opioids class has emerged as one of the fastest growing groups. Indeed, in the period 2014 to 2016, the largest percentage increase in NPSs was observed in the group of novel synthetic opioids (NSOs) (2% of all NPSs in 2014 vs. 4% of all NPSs in 2016)^{8,9}, reaching the 12% of the total NPS reported in early 2023.

1.2 New Synthetic Opioids (NSO)

The origin of the rapid spreading of this class of substances could be considered closely related to the so called “opioid crisis”. With this term, clinicians and toxicologists defined a period from ‘90s years divided in three waves. The first one was characterized by an over prescription of commonly use opioid for pain treatment (e.g. oxycodone), leading to the increase of opioid abusers. The increased

presence of heroin (second wave) led to the trigger of the third wave with fentanyl-contaminated drugs and the consequent development of different fentanyl analogs to increase the potency and circumvent scheduling¹⁰. By the end of 2020, more than 30 fentanyl-related substances had been scheduled¹¹. These compounds were used as stand-alone products, adulterants in heroin or constituents of counterfeit prescription medications¹².

As concerns the definitions, *opiates* include molecules of natural origin, such as morphine and codeine, and some semisynthetic compound with morphine-like structure. In contrast, the term *opioid* is broadly used to describe compounds that act at opioid receptors (including opiates, endogenous peptides and compound with chemical structure different from morphine but with similar effect).

The mechanism of action of these new drugs is strictly related to the opiate prototype, morphine. This molecule derives from poppy plant *Papaver somniferum*, representing one of the most ancient plant-derived medications. The produced effects are analgesia, euphoria, drowsiness, miosis and cough suppression, but at high dosage morphine blocks the respiratory center in brain, causing respiratory depression and death¹³.

Opioid effects are mediated by three classical G-coupled protein receptors: mu- (μ), delta- (δ), and kappa- (κ) opioid receptors, also called MOR, DOR, and KOR, respectively. Among these opioid receptors, MOR was revealed to be the main receptor for both the analgesic and adverse effects of morphine. When this molecule binds to MOR, it causes the dissociation of the α -GTP subunit from the β -subunit complex. The α -subunit inhibits the synthesis of proteins, including the endogenous opioids, through the blockage of the protein kinase which usually activates the transcription factor with phosphorylation. In addition, the β -subunit complex will indirectly inhibit these voltage-dependent calcium channels and block the release of pain neurotransmitters such as glutamate, substance P, and calcitonin gene-related peptide from the nociceptive fibers, resulting in analgesia^{14,15}.

1.2.1 The emerging problem of NSO

In the opioid crisis context, we are nowadays probably facing the fourth wave, characterized by fentanyl analogs and non-fentanyl synthetic opioid responsible for most fatal opioid overdoses. The major issue related to the use of these substances is that little is known about their pharmacological and toxicological characteristics, such as the mu-opioid affinity or the naloxone doses required to treat overdose.

Their potency is not considered by drug-abusers, leading to overdose for example in case of use of fentanyl, which was estimated to be from 50 to 100 times more potent than morphine¹⁶. In some case, these drugs are used as adulterant in illicit street-drugs and even the user is not aware about the presence of substances mixed with the commonly used drug. Moreover, some NSOs are “failed” medications, never marketed due to their adverse effects like addiction.

The proliferation of NSOs is a worldwide problem that requires multilateral approaches; surveillance and monitoring programs are fundamental to control public health challenge. The shared information between nations could help the prevention and the possible treatment of overdoses¹⁵.

2. ANIMAL MODELS

As toxicologists, the main goal of the research is to deeply understand how exogenous compounds act and which are the effects that they produce. In this way and especially in the context of NPS spreading, knowledge of their metabolism is crucial for developing analytical methods for their detection¹⁷. Controlled human studies would be best suited but, because of ethical reasons and lack of preclinical safety data, they are not practicable^{17,18}.

To this aim *in vitro* studies have been employed; examples are assays performed with cell (i.e., human hepatocytes, human liver microsomes) or *in silico* prediction studies. However, these techniques suffer for the high cost, the requirement of highly specialized personnel and instrumentation and they also lack typical components of a living organism. For this reason, the *in vivo* assays could overcome lots of these disadvantages, giving important data about drug absorption, distribution and toxicity, easily comparable to human.

Rodents represent the most used *in vivo* animal model in pharmaco-toxicology; however, they still exhibit complex, time consuming and expensive procedures needed for authorization¹⁹.

On these grounds, researchers investigate for alternative animal species to overcome these issues, but with characteristics as much as possible representatives for higher vertebrates, looking for high conservation of genes, receptors and molecular processes²⁰.

In the last decades, a new animal model has been proposed for this purpose, zebrafish.

2.1 Zebrafish

Zebrafish, or *Danio rerio*, was firstly described in 1822 by Hamilton and it belongs to the Cyprinidea family. The name *Danio* derives from the word “dahni” of Bengali language which means “of the rice field”. Zebrafish is a tropical species

originated from South Asia (particularly from India, Bangladesh and Nepal), which populates the shallow and stagnant waters of the Ganges.

D. rerio body is fusiform with a terminal oblique mouth, with the lower jaw protruding further than the upper. Adult zebrafish rarely exceeds 40 mm and has two characteristic stripes first form centrally with subsequent stripes being added above and below²¹. Also, a “leopard” danio exists and, according to different genetical analysis performed, it is now known to be a spontaneous mutation of the wild type, with homozygotes displaying a spotted pattern, while heterozygotes have stripe pattern²². The discrimination between male and female is not easy, although males tend to be more yellow, and female could have a more swollen abdomen due to the presence of eggs²³.

Zebrafish began to become a protagonist as animal models in 1981, when Streisinger *et al.* pioneered its use in molecular genetics to the study of vertebrate. Moreover, Kimmel *et al.* published the description of developmental stages and cell differentiation²⁴. Starting from that period, it has become a model organism widely used in numerous research fields in addition to genetics, such as developmental biology, toxicology, the study of new drugs and diseases²⁵. The beginning of zebrafish establishment as animal model, compared to other animal used in research, is due to lot of advantages.

Among all these, it is firstly important to mention the rapid development, with the formation of larvae in 72 hours²⁶. Females can spawn every 2-3 days and a single clutch may contain several hundred eggs. The formation stages could be visually followed without invasive techniques because eggs are transparent. This aspect could be really exploited in different kind of research assays. Specifically, from 10 to 24 hours the organogenesis occurs: at 10 hours post fertilization (hpf) the first somite appears; at 12 hpf it starts the genesis of the cephalic region (telencephalon, diencephalon, mesencephalon and rhombencephalon). At 18 hpf the embryo shows the first contractions, symptom of the presence of functional muscle structures. At this point the embryo has a very curved appearance, wrapped around the yolk sac as depicted in figure 1. After 48 hours, the second phase of organogenesis begins: it looks straightening and the functional differentiation of the organs, the vascularization, the formation of the fins, the digestive tract starts, and the heartbeat

is perceptible. During the early stages of embryonic development, zebrafish embryos are covered by a chorionic membrane (the shell) which is lost after about 72 hours²⁴.

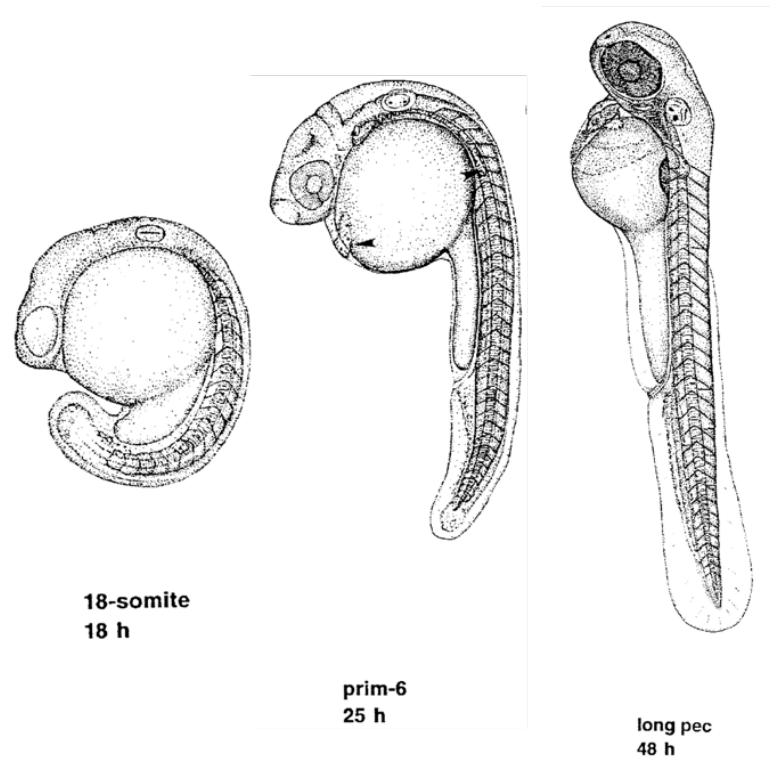


Figure 1: Final stages of zebrafish development at 18, 25 and 48 hours post fertilization²⁴.

At 5 days post fertilization (dpf) the heart, liver and other organs are fully developed, at 6 dpf the larvae begin to feed, at 30 dpf they are already considered juvenile and reach sexual maturity at approximately 90 dpf²⁵. This rapid embryo development is extremely advantageous in the research field: for mice, for example, these times are much longer. Indeed, gestation period for mice is estimated to be 18-22 days²⁷.

Moreover, until the 5th dpf (i.e., the independent feeding stage) zebrafish is not considered laboratory animal according to the Directive 2010/63/EU of the European commission, making possible animal studies with unknown compounds, which are rarely approved by ethics committees in compliance with the reduction to the minimum the sacrifice of animals. On the contrary, animal studies with mice require Ministerial approval, which often has long timelines, thus delaying then the

start of the experimental study. In addition, with mice, handling is more complex and required highly specialized personnel.

Another advantage of zebrafish, over mammals, is the small dimension of this animal model, which reduces the housing space, and the husbandry cost, allowing also high-throughput analysis²⁰, which would be strongly limited with mammals.

Zebrafish, although ideally distant from the evolutionary scale point of view, has a relatively high genetic homology with mammals and human. The nucleotide sequence seems to be for 70% similar to that of human gene and 84% of genes involved in human disease have a counterpart in zebrafish²⁸. This homology includes also genes coding for metabolic enzymes, thus allowing to perform metabolism studies.

All of these reasons support the hypothesis to use it as a possible new translational animal model.

2.1.1 Morphological assay in zebrafish

Zebrafish, and zebrafish larvae in particular, could be exploited for the evaluation of the toxicity of different type of molecules, such as pollutants, toxicant agents or drugs. Simply through waterborne exposure, it is possible to obtain information on the effects caused by acute or chronic exposure to exogenous compounds. The test could be performed by mere observation of macroscopical damage with an optical microscope.

Another possibility to assess toxicity is to study substances' sites of action by identifying apoptosis. For this purpose, some dyes can be used to determine cell death and also to quantify it. An example is represented by the acridine orange staining assay, employed in this thesis. The acridine orange is a nucleic acid intercalant able to emit green fluorescence when bound to double-strand DNA. Thus, this assay is performed to evaluate DNA accumulation in the extracellular matrix in case of cell death.

2.1.2 Metabolic studies in zebrafish

Studies have already been performed using zebrafish to deeply understand the elimination of xenobiotics belonging to different research field, like environmental

pollutants, drug discovery or toxicological evaluations. However, little is still known in the use of zebrafish as animal model in metabolic studies. The possibility to perform both phase I (N-demethylation, oxidation, O-demethylation and N-dealkylation) and phase II (sulfation and glucuronidation) has been demonstrated for the presence of enzymes responsible for these reactions highly conserved in relation to human²⁹. Cytochrome P450 (CYP) enzymes are responsible, in human, for phase I metabolites and they seem to have direct orthologs in zebrafish, suggesting that the metabolic pathways could be similar. Nevertheless, there are some CYPs present in zebrafish that lack the corresponding protein in human (like CP2AE, CYP1C and CYP2X)³⁰: however, among the 94 CYP zebrafish gene found, CYP 5- 51 and CYP 1, 2, 3 (relevant for drug and pollutant elimination) have the human counterparts (Hill, 2013). In addition, it could happen that for the same substrate the metabolite ratio is different²⁵.

Regarding phase II metabolites, in humans the most common biotransformation involved glucuronidation (UDP-glucuronosyltransferase, UGTs) and sulfation (sulfotransferase, SULTs).

In zebrafish, a total of 45 UGT gene were identified, showing close feature with mammals³²: their expression is increased in the period between 3 to 5 dpf in liver and intestine of female and male zebrafish. Also regarding SULTs, the majority of these genes belongs to the SULT1 subfamily, like in human³³.

All of these considerations lead to the conclusion that zebrafish larvae could be tested in the framework of xenobiotics metabolism, since increased knowledges could be fundamental in the determination of possible analytical targets in forensic toxicology.

2.1.3 Behavioral assays in zebrafish

Considering that genetic pathways controlling signal transduction are highly conserved between zebrafish and humans³⁴, also zebrafish is gaining in popularity in parallel with other animal models. Lot of studies focus their attention on testing its cognitive ability, including learning and memories, and how spatial and visual changes could interfere in its behavior. Thus, it could be particularly useful for determining the mechanisms of action of various classes of psychoactive drugs.

Therefore, different behavioral test, also called paradigm, have been developed during years.

An example is the *open-field test*, originally created for rodents³⁵ but adapted for zebrafish larvae³⁶. It basically consists of introducing an animal into a plain arena (without previous contact with it) and of observing its behavior across a specific range of time in order to register the exploratory activity, expressed as distanced moved in the unit of time. This activity is decreased during the trial, determining a basal state, defined as *habituation*³⁷.

Another approach in the field of behavioral studies involves the so-called *scototaxis*, defined as the natural preference of zebrafish to swim in dark environment. This aspect allows for the study of anxiety-like behaviors, comparable to a human anxiety state. In this context, a new tool was established for the first time by Blaser, who developed a light-dark tank³⁸. During his experiments, Blaser confirmed the tendence of adult zebrafish to be confined in the dark side, displaying freezing behavior when forced to stay in the bright side. On these bases, a new paradigm was developed also for larvae, the *startle test*. With this term we refer to a sensorimotor universal response to a stimulus, which can be tactile, visual or acoustic. The consequence is a rapid and protective reaction to this impulse. In our case, a visual startle test was applied: a larva was placed in a well of multi-well plate inside a close chamber equipped with light and infrared camera. After a brief habituation to the environment, a transition from light to dark was carried on^{39,40}: this stimulus was repeated during the behavioral test and the resulting changes in the distance moved were recorded.

3. ANALYTICAL TECHNIQUES

3.1 Liquid Chromatography coupled with mass spectrometry (LC-MS)

The liquid chromatography (LC) is a technique used in different field of research for the separation of compounds within a mixture according to the interaction and the affinity between a mobile and a stationary phase.

A liquid chromatograph instrument is generally composed by an injector, a separative compartment (column) and a detector as depicted in the figure 2.

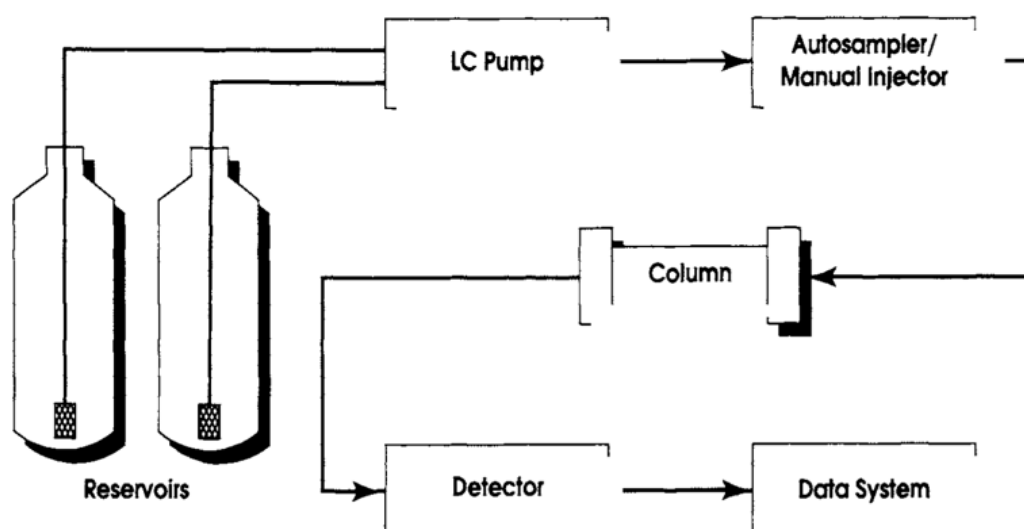


Figure 2: Schematical representation of a high-pressure liquid chromatograph⁴¹.

The *injector* is the element that allows for the introduction of the sample into the flow stream of the liquid phase. It is specifically designed to place a liquid sample into the solvent stream with a perturbation as little as possible. In order to do this, an autosampler was developed, which also keep samples at a specific controlled temperature.

The *separation* occurs in column packed with a solid adsorbent, the stationary phase; when the mobile phase passes, the components are attracted to the adsorbent surface of the stationary phase depending on their unique structural features and

interaction with the eluents. The efficiency of the process is strictly related to the nature of the adsorbent solid used and the polarity of the mobile phase solvent. Each component of the sample is eluted at a different time, the retention time (RT): the elements with a large distribution constant, which are more attracted to the stationary phase, will be more strongly retained, and migrate at a slower rate than others with higher affinity for the mobile phase.

The technique was initiated in 1906 with Tswett's work and at the very beginning was based on simple manually filled columns: from this, several progresses have been made, especially regarding improvements in resolution obtained with solid phase of smaller diameters and consistent particle size, together with pumps capable of producing high pressure with uniform flow. Nowadays, the separations generally take place in column made of stainless steel which can be differentially packed with silica or polymers, functionalized in different ways according to the chemicals that are being analyzed. Silica is one of the most popular adsorbent materials for its high sample capacity. Depending on the diameter, analytical columns are classified into standard columns (typical internal diameter 4.6 or 4.0 mm), semi-micro columns (typical internal diameter 1–2 mm) and micro or capillary columns (internal diameter 0.1–1.0 mm)⁴².

The most used LC application is the reversed phase (RP) chromatography. This is characterized by silica gel particles modified with a lyophilic layer of alkyl groups bound to silanol (Si-OH) groups. Long alkyl chains, typically C18, bind stronger to organic molecules of low polarity while highly polar or even ionic analytes pass by. On the other hand, shorter alkyl groups (like C1 to C8) have lower retention for low polarity analytes. Overall, reversed phase chromatography leads to retention times in the order nonpolar > polar > ionic.

The most important features to consider are the particle diameter, the pores dimension, the length, and the internal diameter of the column. All these elements can affect the efficiency and the resolution of the chromatographic separations. In particular, the particle size significantly affects the separation efficiency. The larger the bead size is, the lower is the pressure affects the system. Separations performed for preparative analysis benefit with beads sizes in the 3–5 μm range, while smaller ranges are usually specified for mass spectrometry (MS) detection. Moreover, a

uniform distribution of the packing minimizes the presence of air bubbles and dead volumes throughout the entire experiment when the solvents flow.

As regard separations, the choice of the mobile phase strongly depends on the type of analytes to detect. However, ideally the mobile phase should be high purity, low cost, low viscosity, and it should be a solvent for the samples. Usually, a mixture of aqueous and organic eluents such as methanol or acetonitrile and additives like buffer are commonly used⁴³, since the pH can affect ionizable compounds in organic acids or organic bases. The solvents may also be modified during separations in order to change the polarity by increasing the organic phase. The elution mode can be set as isocratic elution or as gradient elution: in the first case, the chromatographic conditions are kept constant during the elution; in the other case, there is a gradual increase of the elution power, by increasing the concentration of the organic phase.

Another important element in an LC system is represented by the *pumps*: their main function is to force the liquid (mobile phase) at a specific flow rate, expressed as mL/min. The solvent passes using high pressure: this helps to maintain a specific flow rate which contributes to determine how fast a chemical will migrate through the column.

Finally, the *detector* is the device used to detect the eluted component of the mixture. In forensic toxicology, the most common detector coupled with LC is the mass spectrometer.

The mass spectrometry is an analytical technique used to identify ionized compound base on their mass-to-charge ratio (m/z). The technique originated from studies conducted by Thompson and Aston, allowing for the development of the first mass spectrometer in 1919. This instrument used gas discharge tubes to generate ions, which were then passed through parallel electric and magnetic fields. The ions were then detected⁴⁴.

Nowadays, mass spectrometry is one of the most frequently employed technique in many different analytical fields, including forensic toxicology.

By using LC-systems in combination with MS-detectors, thermolabile, polar and volatile compounds can be easily determined. In a typical MS procedure, a sample

is ionized, and molecules are broken into charged fragments. Ions are then separated typically by accelerating them due to an electric or magnetic field and detected by a system capable of detecting charged particles. Results are displayed in spectra with the relative abundance of detected ions as a function of the mass-to-charge ratio. The atoms or molecules in the sample can be identified by correlating known masses to the identified masses or through a characteristic fragmentation pattern. A mass spectrometer (Figure 3) could be schematically described as composed by an ion source (that generates ions from the sample), a mass analyzer (which separates ions according to their m/z ratio), and a detector (to count ions and to measure their abundance), which are operated under high vacuum.

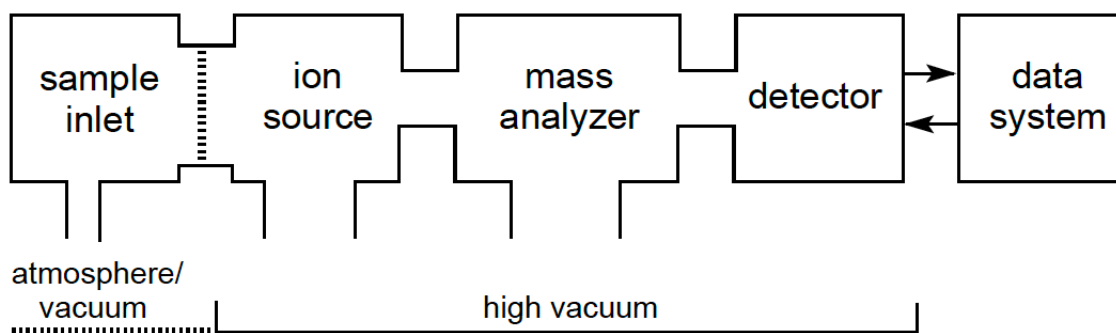


Figure 3: General scheme of a mass spectrometer⁴⁵.

3.1.1 Ionization sources

The ion source is the part of the instrument that allows the formation of charged species from a neutral one: this is achieved through the removal/addition of electrons or through the removal/addition of the protons, according to the method utilized.

In general, the ionization systems could be divided into *hard*, because they work at high energy, and they cause a high fragmentation or *soft* characterized by low energy and a lower number of fragments. The mostly used sources in LC-MS are soft system, like the Atmospheric Pressure Chemical Ionization (APCI) and the Electro Spray Ionization (ESI). According to the type of analytes, an ionization technique could be preferred compared to another one. ESI is the most common ionization sources in LC-MS and the one used in the present work.

3.1.1.1 The Electro Spray Ionization (ESI) technique

The ESI ion source consists of a capillary needle with an applied voltage, through which the sample is injected from the LC instrument. The needle probe is surrounded by a gas (nebulizing gas, usually nitrogen) which promotes the formation of droplets and the evaporation of the solvents. Vaporization increases the charge density on the surface of the droplets and the electrostatic repulsion increases, together with the surface tension, until the droplet undergoes “coulombic explosion” (fig. 4). Repulsion between the charged ion and other charges of the small highly charged droplet leads to the emission of singly or multiply charged ions into the gas phase. ESI can operate in either positive or negative mode, leading to the formation of $[M+H]^+$ and $[M-H]^-$ respectively. It is considered a soft ionization technique, because there is very little fragmentation that yields intact analyte ions with one or more charges.

On one of the main advantages of ESI interface is that it permits MS analyses of small molecules such as drugs of abuse, or larger, including proteins.

On the other hand, one limitation of ESI is its susceptibility to matrix effects that can cause undesired ionization suppression or enhancement phenomena. Matrix effects can vary between specimens affecting the relative abundance of ions in the mass spectrum, potentially producing inaccuracy in quantification.

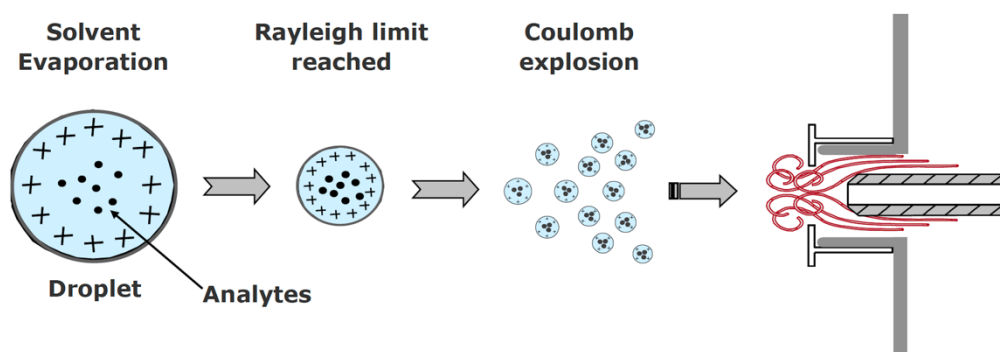


Figure 4: Droplet formation in an ESI ionization source⁴⁶.

3.1.2 Mass Analyzer

The mass analyzer is the part of the instrument that separates ions according to their mass-to-charge ratio: the key specifications are sensitivity, mass measurement accuracy and resolution. The sensitivity is the ability of the instrument to detect the

ions. Mass accuracy is the deviation of the measured mass value from the true value. The closer the obtained values are to the reference value, the higher the accuracy. Ultimately, mass resolution is the ability to separate two ions with similar masses, hence resolving power is the ability of the instrument to resolve adjacent peaks. Analyzers are usually considered at low resolution if R is less than 5000 and high resolution if R is greater than 5000.

According to the final aim of the analysis, it is possible to employ low- or high-resolution mass spectrometry (HRMS). High-resolution mass spectrometers tend to be expensive and generate large quantities of data, which are not necessary for routine analyses that can be processed using low-resolution mass spectrometry. For this reason, low resolution mass spectrometers are commonly present in research laboratories and used for identification and quantification in target analysis.

Instead, HRMS is a useful tool to analyze complex sample matrices and for the relative structural identification, in conducting nontargeted analyses⁴⁷.

For these instruments, the resolution and the mass accuracy are of great importance. Particularly, mass accuracy is expressed as parts per millions (ppm), and it is given by the following relationship:

$$ppm = \frac{\text{Observed mass} - \text{theoretical mass}}{\text{theoretical mass}} 10^6$$

In HRMS, the resolution required to separate two ions with masses M and $M+\Delta M$ is defined by the ratio: $R=M/\Delta M$ and indicated as Full Width Half Maximum (FWHM). The narrower the peak obtained, the more the ions can be separated.

Thanks to these improved characteristics, HRMS can identify m/z with four decimals, allowing to discriminate between different molecules even before the fragmentation. For this reason, high-resolution spectrometers have to be highly calibrated with known masses before the analysis.

Various types of mass analyzers are employed in forensic toxicology: the most widely used for low resolution are quadrupole or ion trap analyzers, while for high resolution the Time Of Flight (TOF). In any case, it is possible to combine these types of analyzers in order to increase resolution and accuracy^{45,48}. In this thesis, the quadrupole and the TOF analyzer will be explored in depth, as they are

components of the hybrid instrumentations used. Moreover, an orbitrap instrument was employed, and it will be discussed in future chapters.

3.1.2.1 Quadrupole analyzer

The operating principle of this type of analyzer is the separation of ions with different m/z by exploiting their different stability within a quadrupolar radio-frequency electric field. It consists of four cylindrical metal rods, having the same diameter and length, placed parallel according to the vertices of a square (see figure 5). The electric field is generated when a radio frequency (RF) voltage is applied between one pair of opposing rods within the quadrupole.

Only ions of a certain m/z will have a stable flight path through the quadrupole in the resulting electric field; all other ions will have unstable trajectories and will not reach the detector⁴⁸.

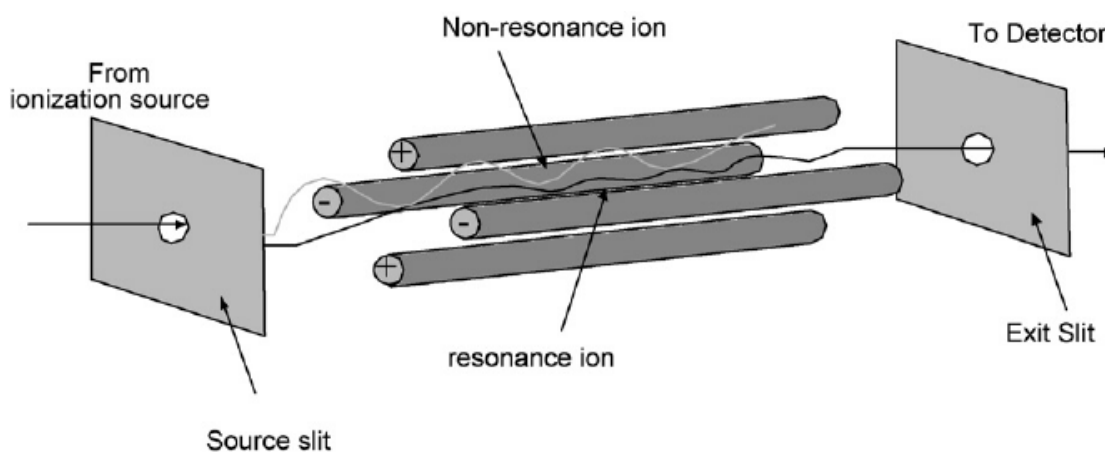


Figure 5: Schematic representation of a quadrupole⁴⁹.

The quadrupole can be also available as triple quadrupole mass spectrometer (QqQ), in which three sets of quadrupole analyzers are used in sequence. The first quadrupole is acting as a mass filter for specific ion to the second quadrupole, which represents the collision cell, where that ion can be selectively broken into fragments. The third quadrupole also acts as a mass filter, to transmit a particular fragment ion to the detector.

Another possible combination is the Quadrupole-Time Of Flight (QTOF), analyzer which combines the sensibility of the quadrupole with the accuracy of High-

Resolution Mass Analyzer (HRMA). This hybrid instrument was used for part of this thesis project.

3.1.2.2 Time of Flight (TOF) analyzer

In the time-of-flight analyzer, ions with different m/z values are separated in time as they fly along a field-free path of known length. The ions are formed in pulsed mode, and the analyzer measures the time necessary for them to reach the detector. Ions having different masses, but equal kinetic energy will have different velocities and they will travel the fixed distance at different times; smaller ions will reach the detector sooner than larger ones. In fact, the kinetic energy of an ion is directly proportional to its mass and velocity according to the relationship of kinematics: $E_{\text{kinetic}} = \frac{1}{2} m v^2$. The ion with lower mass moves faster and it will reach the detector first, followed by the intermediate mass ion and finally the ion with high mass. In this way, the ions can be temporally resolved⁴⁵.

The main advantages of TOF instruments are that in theory it is possible to have an unlimited m/z range, having a complete mass spectrum within several tens of microseconds. Moreover, the transmission of a TOF analyzer is very high, thus resulting in high sensitivity⁴⁵.

TOF instrument could be linear, or it could also work with a reflectron (ReTOF) (Figure 6), which it acts as an ion mirror that focuses ions of different kinetic energies in time. The performances are improved using two-stage or multistage reflector design. This aspect largely increases the resolving power of the instrument. In this thesis, a 6540 Accurate-Mass QTOF spectrometer (Agilent Technologies, Palo Alto, CA, USA) was used.

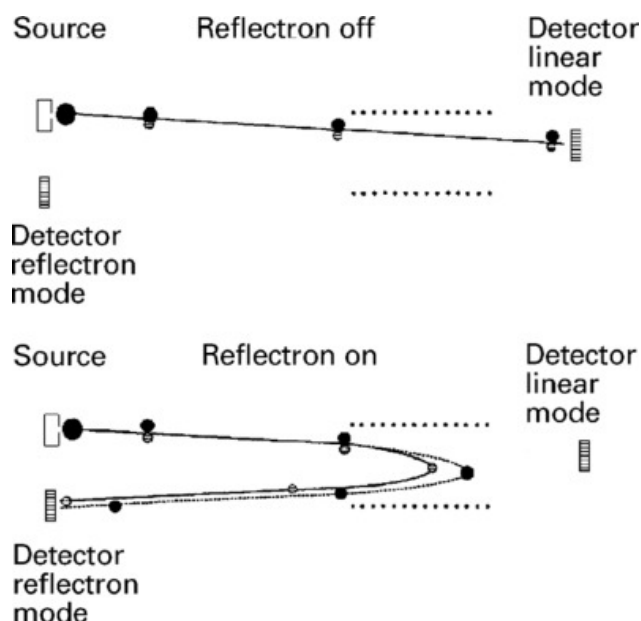


Figure 6: Schematic diagram of the procedure of MS-MS with reflectron TOF instrument⁵⁰.

3.1.2.3 Orbitrap analyzer

The orbitrap is a mass analyzer consisting of ion trap but there is neither a radio frequency nor a magnet to keep the ions inside. Commercially available since 2005 from Thermo Fisher Scientific company, the Orbitrap™ originally derives from a device to trap ions based on a straight wire along the axis of a cylindrical electrode developed in 1923 by Kingdon⁵¹. Later, Knight modified the external electrode: this machine was able to trap ions and release them to a detector, but it could not discriminate between different m/z ratio. The first proposal for a mass analyzer which exploit this concept was elaborate by Makarov in 2000⁵². This analyzer was called *orbitrap* and it can be considered a refined version of the trap of Kingdon, modified by Knight. Nowadays the instrument is equipped with a fusiform central electrode and an external barrel electrode (Figure 7 (a) and (b) respectively). The ions are injected inside, and they remain trapped thanks to an electrostatic field. The electrostatic attraction to the central electrode is counterbalanced by a centrifugal force originating from the initial tangential velocity of ions⁵³. Ions move in spirals around the central electrode: the trajectory has two components radial (long r) and axial (long z). It can be demonstrated that the axial oscillation frequency is given by: $\omega = \sqrt{k \left(\frac{q}{m} \right)}$ and it is inversely proportional to the square root of m/z (k is a

constant that incorporates the characteristics of the electric field due to the particular shape of the two concentric electrodes).

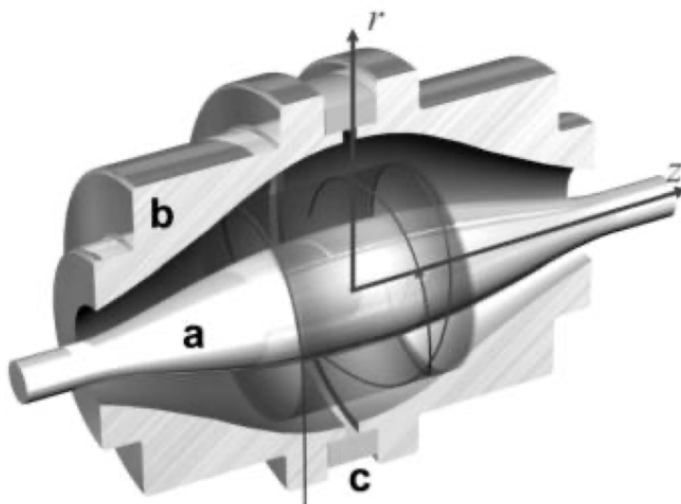


Figure 7: A cut-away model of the orbitrap mass analyzer. Ions are moving in spirals around a central electrode (a). An outer electrode (b) is split in half by an insulating ceramic ring (c)⁵³.

The measurement of m/z of the different ions present in the trap is done using the Fourier transform, as for Fourier transform ion cyclotron resonance (FT-ICR), even if in this case it is not necessary to apply a magnetic field, resulting in a lower cost of the instrument⁵⁴.

In this thesis project, an Orbitrap Fusion™ Lumos™ Tribrid™ Mass Spectrometer (Thermo Fisher Scientific, Waltham, USA) was used. It ensures scan speeds of up to 20 Hz and a top mass resolution of up to 500,000 (FWHM) at m/z 200, according to the indications of manufacturer⁵⁵. With this instrument, an auto MS/MS can be performed in simultaneous with the full scan (single run), meaning that above a specific threshold a fragmentation is applied.

3.1.3 Detector

The final element of the mass spectrometer is the detector. Mass detector mainly detect the current signal generated from the passes or incident ions which are absolute or relative concentration of each analyte. Detector output after amplification is traced on a recorder. Results are displayed as spectra of the relative

abundance of detected ions as a function of the mass-to-charge ratio. The detector with desirable properties in mass spectrometer should have:

- High amplification,
- Fast time response,
- Low noise,
- High collection efficiency,
- Low cost,
- Narrow distribution of responses,
- Same response for all masses,
- Large dynamic range,

Different types of detectors are available in the market, the most important of which are Ion detector, Conversion Dynodes, Cryogenic detector⁵⁶.

3.1.4 Acquisition modes

The mass analyzers can operate in different modes: the two most important, which are also carried on in the current work, are:

- Scanning mode: monitoring all the m/z present in the sample.
- Target MS/MS: monitoring a specific targeted ion and performing a fragmentation.

3.1.4.1 Full scan mode

The full scan mode is used when it is necessary to recognize the greatest number of compounds in a sample, it is used when a new sample is being analyzed for the first time, or when a new analytical method is being developed. In this mode, the analyzer sequentially transmits to the detector all masses formed in a range selected by the operator. The entire mass spectrum of what is being eluted is thus obtained moment by moment. The resulting chromatogram is given by the total ion current (TIC) as a function of retention time. This type of acquisition can be applied for screening or confirmation method, or in accurate mass screening procedure.

3.1.4.2 Target MS/MS

In a target analysis, the first step is characterized by the isolation, performed by the first analyzer (MS1) which acts as a “filter” among all the possible ions generated. The selected ion is then fragmented, and the fragments generated are separated from the second analyzer (MS2), according to their m/z .

Fragmentation is very useful in cases where it is necessary to recognize the structure of an unknown molecule or in analyses where the substance to be investigated is found in very low quantities (for example, for metabolites). In the current thesis project, both of the instrument utilized (QTOF and orbitrap) can acquire in full scan mode and in target MS/MS.

3.2 DanioVision tracking system

The DanioVision system consists of an observation chamber, the EthoVision 17 XT video tracking software and a temperature control unit (see figure 8). The temperature control unit allows to set a water flow at constant temperature (28.5°C) under the multi-well plate in the observation chamber, with a water level regulated by a filling-draining system. In the observation chamber, there is a white light source, controlled by the tracking system (which can be adjusted in terms of intensity) and an infrared camera which can monitor the activity even when the light is off.



Figure 8: DanioVision apparatus: in the left the observation chamber (a), then represented open with the infra-red camera; in (b) the temperature control unit.

The system is compatible with multi-well of 6-12-24-48-96 well plate: one larva is placed in each well and the EthoVision 17 XT software calculates each subject's activity as the distance covered in each minute of the test. To obtain these data, it is necessary set the *arena*, that is the region in which larvae can swim. Different behavioral test can be carried out by simply modifying the setting of the test (example in terms of test duration, visual or acoustic stimuli).

4. AIMS OF THE THESIS PROJECT

As already described, the emergence of the New Psychoactive Substances is nowadays a problem of global concern as above described. The continuous appearance and diffusion of compounds with related chemical structure but unknown potency and effects still pose a significant challenge for forensic and clinical toxicologists. In such a complex situation, the most important aspect is to gain knowledge on their pharmaco-toxicological characteristic in a rapid way to keep up with the modification applied to the chemical structure to evade legislation. Although rodents represent a well-established *in vivo* animal model, they show some problems hindering ethical issues in the use of laboratory animals and the related complex, time-consuming and expensive procedures. For these reasons, in the last decade zebrafish have emerged as an attractive alternative animal model for its unique properties such as small size, high prolificacy, rapid maturation and low costs.

To this purpose, the general idea is to set up a new strategy involving the use of zebrafish as new screening tool for the rapid study of NPS. In particular, we decided to use zebrafish larvae, since until the fifth day post fertilization is not considered a “sensitive” animal and it can be used without the Ministry approval, resulting in a reduced experimental time. However, since the animal is still considered relatively new in the toxicological field and absolutely new in our laboratory in Verona, we first started with the comparison of zebrafish with mice through the collaboration with the Pharmacology Unit of the University of Ferrara. In order to do this, we initially decided to optimize the experimental protocol by testing fentanyl, a known molecule synthesized in 1960 as medicinal drug but recently gained in popularity as recreational drug. The study involved behavioral and metabolic assay to confirm data on effects and toxicity of this drug.

After setting up the protocol with fentanyl, the zebrafish model in comparison with mice had been applied to the toxicity evaluation of two relatively new fentanyl analogs, namely ocfentanil and 2-furanylfentanyl. On the bases of the promising results obtained with the studied fentanyls, the study has been extended to the

evaluation of the metabolic pathways in zebrafish larvae (ZL) of nine new synthetic opioids (namely AP-237, 2-methyl-AP-237, isotonitazene, metonitazene, etodesnitazene, N-pyrrolidino etonitazene, butonitazene, flunitazene and metodesnitazene) to clarify the metabolites of these new drugs to be analyzed in biological samples collected from users.

5. EXPERIMENTAL PART

5.1 Animal Husbandry and Ethic Statement

In the present study, the experimental protocols applied on zebrafish larvae were performed at the Centre for Experimental Research (CIRSAL) of the University of Verona in accordance with the Italian and European Legislations (Directive 2010/63/EU) with permission of the Animal Welfare Body of the University of Verona. Zebrafish embryos were obtained from natural spawning of AB-strain wild-type adults raised according to standard protocols²⁴ at a constant temperature of 28°C. Fluorescent lamps provided illumination with a 14:10-h light-dark cycle. Adult zebrafish were fed four times a day, twice with *Artemia nauplii* and twice with dry food (Zmsystems, Winchester, UK). Fish were kept at a maximum density of 17 exemplars in 3.5-lt tanks. For reproduction, pairs of adult zebrafish were transferred into a breeding cage: the two breeders were divided by a transparent partition until the following day, when the partition was removed allowing spawning. Embryos were collected and raised in a Petri dish in fish water medium (1 mM calcium sulphate, 1.2 mM sodium bicarbonate and 0.02% (w/v) Instant Ocean).

The experimental protocols performed in mice were compliant with the UK Animals (Scientific Procedures) Act of 1986 and relative guidelines and with the new European Communities Council Directive of September 2010 (2010/63/EU), a revision of the Directive 86/609/EEC. Protocols were approved by the Italian Ministry of Health (license n. 335/2016-PR) and by the Animal Welfare Body of the University of Ferrara. According to the ARRIVE guidelines, all possible efforts were made to minimize the number of animals used and animals' pain and discomfort. Adult male ICR (CD-1®) mice (about 12 weeks old) weighing 30–35 g (Centralised Preclinical Research Laboratory, University of Ferrara, Italy) were group housed (5 mice per cage; floor area per animal was 80 cm²; minimum enclosure height was 12 cm), exposed to a 12:12-h light-dark cycle (light period

from 6:30 AM to 6:30 PM) at a temperature of 20–22° C and humidity of 45–55% and were provided ad libitum access to food (Diet 4RF25 GLP; Mucedola, Settimo Milanese, Milan, Italy) and water.

5.2 ZL applied in the study of behavioral effects and metabolism of fentanyl

The first year of my PhD was focused on testing zebrafish larvae as possible new animal model. The study concerned the use of a relatively known compound (i.e., fentanyl). Data were compared to those obtained at the Pharmacology Unit at the University of Ferrara by testing in parallel fentanyl in mice.

5.2.1 Fentanyl

Fentanyl was synthesized in 1960 by Paul Janssen for the Janssen Pharmaceutica company, with the intention to produce an analog of morphine drug but with fewer unwanted side effects and a greater analgesic potency. Fentanyl is a monocarboxylic acid amide resulting from the formal condensation of the aryl amino group of N-phenyl-1-(2-phenylethyl)piperidin-4-amine with propanoic acid⁵⁷ (see figure 9).

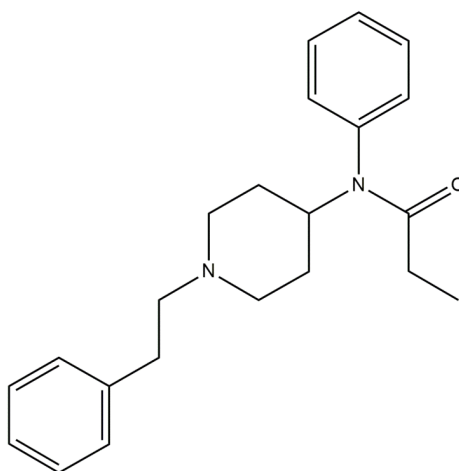


Figure 9: Fentanyl chemical structure.

Thanks to its great lipid solubility, it easily penetrates the central nervous system, having also higher specificity for MOR receptors, short onset and duration of action. Additionally, its potency is considered from 100 to 200 times more potent than morphine. The typical effects, mediated by the μ -opioid receptor, include analgesia, feeling of relaxation and euphoria, miosis, dizziness, fatigue, nausea, vomiting, constipation, and respiratory depression¹⁶. As above-mentioned, it was

firstly produced for medical use, which means as anesthetic drug by injectable formulation⁵⁸. Then, a large demand prompted the development of different formulations (i.e., tablets, spray, patches) for the treatment of chronic cancer pain and/or acute ache. Thus, led to an increased availability of the drug for recreational purpose in the clandestine market, where fentanyl is sometimes used alone but frequently mixed with cocaine, heroin, alprazolam or other sedative substances. In these cases, unintentional intake of a potent opioid such as fentanyl could lead to severe and potentially fatal consequences, particularly in subjects with a low tolerance to opioids¹⁶.

Fentanyl has been internationally controlled, under the 1961 Single Convention, since 1964 for its high potential abuse¹¹. However, for decades after its approval, reports of intoxications were low compared to other opioids. First reports have been described for healthcare professionals such as anesthesiologists, nurse and pharmacists, who had easy access to it. This was considered one of the two main sources of fentanyl for recreational use; the second was represented by the illicit production, which contributed to create the “fentanyl crisis”. Indeed, its synthesis is easier and cheaper and for this reason it is purchased by dealers at low cost and added to heroin with big profits, without the user’s knowledge⁵⁹.

In this context, and considering the ongoing opioids emergency, the present thesis project initially focused on the optimization of a protocol in ZL for the evaluation of behavior and metabolic pathway using fentanyl as target compound. To prove the applicability of the protocol in ZL, the results were compared with those obtained in mice.

5.2.2 Materials and Methods

5.2.2.1 Maximum-tolerated concentrations assay

Embryos were raised in fish water (FW) medium, consisting of 1 mM calcium sulphate (Merck KGaA, Darmstadt, Germany) 1.2 mM sodium bicarbonate (Merck KGaA, Darmstadt, Germany) and 0.02% (w/v) Instant Ocean (Tecniplast, Verese, Italy).

For the maximum-tolerated concentrations (MTC) study, 4 dpf zebrafish larvae were placed in 48-well plates (Sarstedt, Numbrecht, Germany) under waterborne

exposure for 24 h at 28°C. ZL were exposed to fentanyl (LGC Standards, Milan, Italy) concentrations of 1, 10, 50, 100 μM . A vehicle containing 0.34% methanol (VWR Chemicals, Fontenay-Sous-Bois, France) was prepared to exclude any effect of the solvent used for the dissolution of fentanyl standard. To assess the morphological defects, a total of 164 larvae were tested. Larvae were monitored using a model DM2500 microscope connected with a ICC50W camera (Leica Microsystem Vertrieb GmbH, Wetzlar, German). Larvae were evaluated for several developmental malformations, including yolk sac edema and pericardial edema, body axis, trunk length, caudal fin, pectoral fin, pigmentation, jaw and somite deformities according to the abnormalities highlighted by Noyes⁶⁰.

5.2.2.2 Behavioral assay

Larvae were exposed to the selected doses (1 and 10 μM of fentanyl and vehicle) ten minutes before the beginning of the experiment. ZL locomotor activity was recorded by the automatic tracking system, DanioVision (Noldus, Wageningen, Netherlands).

In our experiment, the 48-multi-well plate was placed in the observation chamber, where larvae were exposed to artificial light for 120 min acclimation (*habituation*). Then larvae underwent the *startle test*, with a series of three 10-min dark periods separated by a 10-min period of light: the light-to-dark transition corresponds to the *stimulus*. Overall, the behavioral test consisted of a 180 min recording for each experimental replicate. The assays were conducted by arraying 4 dpf larvae in the multi-well plate (1 larva/well). For behavioral tests 32 larvae were used in each of the following conditions: fish water medium, vehicle, fentanyl 1 μM and 10 μM .

In mice assay, fentanyl was initially dissolved in 2% absolute ethanol (BioUltra, for molecular biology, $\geq 99.8\%$; Sigma-Aldrich) and Tween 80 (Sigma-Aldrich) (2%) and then diluted in a saline solution (0.9% NaCl; Eurospital, S.p.A, Italy). The same solution of ethanol, Tween 80 and saline was also used as the vehicle. Drugs were administered by intraperitoneal injection at a volume of 4 $\mu\text{l/g}$. The doses of fentanyl (0.1–15 mg/kg) were chosen on the basis of a previous preliminary study in mice⁶¹. Changes of the spontaneous motor activity induced by fentanyl were measured using the ANY-maze video-tracking system (Ugo Basile, application

version 4.99g Beta). A single mouse was placed in a square plastic cage (60×60cm) located in a sound- and light- attenuated room and the motor activity was evaluated for 310 min^{62,63}. Four mice were monitored at the same time in each experiment. The distance travelled (m) was measured every 15 min for a maximum of 310 min. Since typically the spontaneous motor activity of the animal progressively reduces over time, posing problems to distinguish whether the immobility of the mouse is due to the action of opioid agonist or to the normal resting behavior of the animal in the open field test, the mice were mechanically stimulated when they were completely stationary in both the vehicle group and the fentanyl group. The mechanical *stimulus* was applied at minute 225, gently touching the back of the mouse with a plastic stick with a rounded tip three consecutive times. For the overall study 56 mice were used. In the *open field test* for each treatment (vehicle or 4 different fentanyl doses, 0.1, 1, 6 and 15 mg/kg) were used 8 mice (total mice used: 40).

5.2.2.3 Metabolic assay

The analytical instrumentation used in the present study was a model 1260 Infinity LC coupled to a 6540 Accurate-Mass QTOF spectrometer (Agilent Technologies, Palo Alto, CA, USA). A gradient chromatographic separation was performed using a C18 Zorbax Eclipse XDB column (2.1 × 150 mm, 5 µm particle size, Agilent Technologies), thermostated at 20°C. The flow rate was set at 200 µL/min. A sample volume of 5 µL was injected. The composition of the mobile phase was as follows: formic acid (Merck KGaA, Darmstadt, Germany) 0.1% in ultrapure water (Elga Veolia Lane End, High Wycombe, UK) as phase A and acetonitrile (Merck KGaA, Darmstadt, Germany) added with 0.1% formic acid as phase B. The gradient elution profile was: 0–2 min 2% B, 2– 13 min linear gradient from 2 to 95% B, 13– 16 95% B, 16 min 2% B. The QTOF-MS was fitted with a Jet Stream electrospray ion source (Agilent Technologies) operating in positive ionization mode. The ion source parameters were heater temperature, 325°C; gas flow, 8 L/min; nebulizer gas pressure, 30 psi; sheath gas temperature, 360° C; sheath gas flow, 12 L/min; VCap, 3750 V; fragmentor voltage, 150 V. Data were acquired in full-scan mode,

within a range of 100–1000 m/z. Fragmentation was obtained on the ions of interest by applying a collision energy of 20 eV.

The same larvae used for the behavioral assay with fentanyl at the final concentrations of 1 and 10 μM were incubated for 24 h at 28°C. Subsequently, larvae were collected separately: they were euthanized with ice water. Afterwards, larvae were snap-frozen by placing them at -80°C . The method developed by Gampfer's⁶⁴ was followed for the extraction of larvae. Briefly, 32 larvae for each vehicle/dose tested were collected together, lyophilized using a SavantTM DNA SpeedVacTM Concentrator Kits (Thermo Scientific, Waltham, Massachusetts, USA) for 60 minutes. Larvae were then extracted by adding 50 μL of methanol, under shaking for 2 minutes. After centrifugation at 12,054g for 5 minutes with Microfuge Lite centrifuge (Beckman Coulter, Ca, USA), the supernatant was transferred in an autosampler vial. The extraction procedure described above was performed on treated larvae, as well as on control larvae in order to exclude the presence of potentially interfering endogenous compounds.

Mice were individually placed inside metabolic cages (Ugo Basile SRL, Gemonio, Varese, Italy) with free access to water and food. Total urine samples were collected in the time interval 0–5 h after the injection of vehicle or fentanyl at 15 mg/kg then stocked at -80°C until analysis. In the urine collection studies for each treatment (vehicle and 15 mg/kg fentanyl) were used 8 mice (total mice used: 16). Urine samples were then simply diluted (1:1000) with ultrapure water and directly injected into the LC-QTOF.

5.2.2.4 Statistical analysis

The statistical analysis was performed with using GraphPad Prism software (Version 8).

As regards ZL, the influence of fentanyl over the time was assessed by means of a two-way Friedman test. The Dunnett's multiple comparison test was used as a post-hoc test to compare the effect of different doses to the vehicle. Furthermore, Kruskal-Wallis and Dunn's multiple comparison tests were performed to evaluate the significant differences between the two experimental phases (basal and

stimulation). Data were represented as mean \pm SEM and significance was set at $p < 0.05$.

Concerning mice, a two-way ANOVA followed by a Bonferroni test for multiple comparisons was performed to analyze the effects of vehicle and fentanyl in different concentrations over the time. Additionally, the comparison of the effects induced by fentanyl on the response to mechanical stimulation was conducted using a two-way ANOVA followed by a Bonferroni test for multiple comparisons. A Student's t-test was used to determine statistical significance between the two groups (see motor changes after mechanical stimulation). Data were represented as mean \pm SEM and significance was set at $p < 0.05$. Data and statistical analysis comply with the recommendations on experimental design and analysis in pharmacology⁶⁵.

5.2.3 Results

5.2.3.1 Maximum-tolerated concentrations assay

Due to lack of information in literature regarding the concentration levels of fentanyl capable of producing an effect on ZL, a study on the MTC was initially performed. ZL were exposed for 24 hours to different concentrations of fentanyl (1, 10, 50, 100 μ M) and morphological malformation were then evaluated.

Although all the treated larvae survived 24h after the exposure, larvae treated with the highest concentrations manifested several morphological malformations. In particular, 100% of larvae exposed to fentanyl 50 and 100 μ M showed an abnormal pericardial edema (PE), yolk sac edema (YSE), jaw defect (J) and spinal curvature (SC), as shown in figure 10. These malformations have already been highlighted for fentanyl^{66,67}, other fentanyl analogs⁶⁴, cannabinoids⁶⁸ and environmental toxins⁶⁹. Furthermore, at those concentrations, larvae seemed to be sedated and suffering, consequently it was decided to reduce the drug concentrations to 10 μ M (which induces malformations only in 1/3 of cases) and 1 μ M (that caused no malformations) for further experiments. In the control groups of larvae, no malformations were observed, thus excluding a toxic effect of methanol in the vehicle (0.34%).

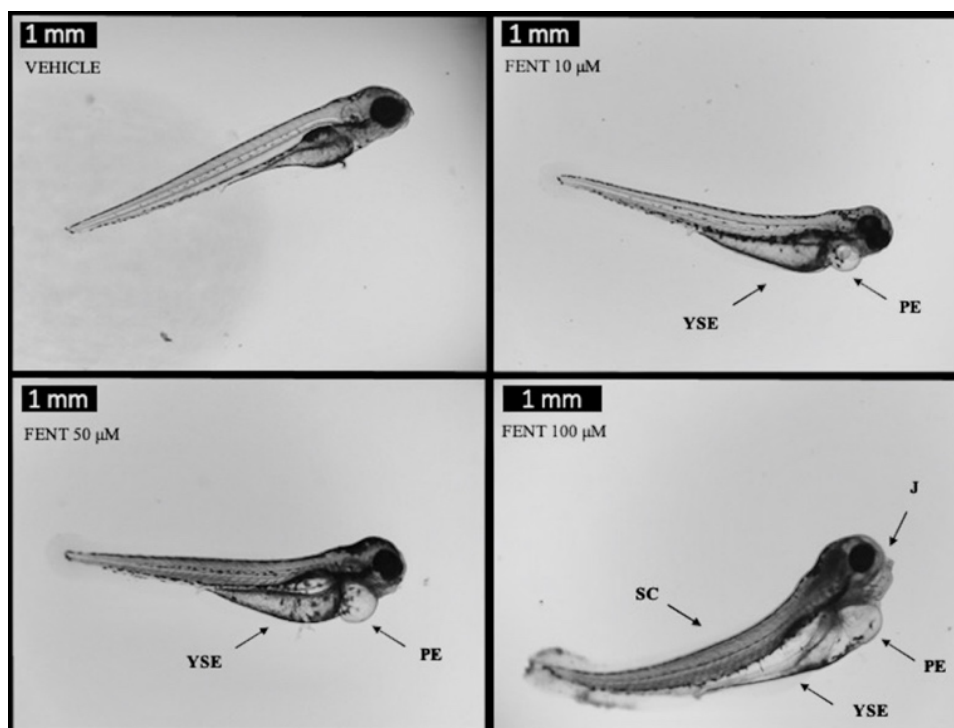


Figure 10: Morphological deformities in zebrafish larvae exposed to fentanyl 10, 50 and 100 μM for 24 h. The observed deformities were pericardial edema, PE; yolk sac edema, YSE; spinal curvature, SC and jaw, J.

5.2.3.2 Behavioral assay

In the present study, a previously validated paradigm⁷⁰ was used to test the acute effect of fentanyl on ZL. The assay measured the basal locomotor activity and the response to a light-to-dark transition, consisting of a stereotyped avoidance response (*scototaxis*), i.e., an increase in activity^{71,72}. Ethovision XT software quantified the total distance travelled by each subject per minute of recording, as a measure of larvae locomotor activity. Firstly, data were analyzed as a whole (Figure 11A) to evaluate the influence of fentanyl. As shown in figure 11A, fentanyl significantly impairs ZL locomotor activity ($p < 0.05$) and at the highest dose (10 μM) consistently reduced the total distance travelled. Since this initial analysis showed variability between treatments and experimental phases, data were split into two main phases, namely basal (1–120 min) and stimulation, represented by the mean of 3 replicates of a stimulus (120–180 min) (Figure 11B). In the basal phase fentanyl decreased larvae basal activity in a dose-dependent manner ($p < 0.05$), while in the stimulation phase only the highest dose (10 μM) caused a decline in locomotion ($p < 0.05$).

As shown in figure 11 (panel C and D), spontaneous locomotion in mice was significantly affected by systemic administration of fentanyl. Effect of the systemic administration (0.1–15 mg/kg i.p.) of fentanyl on the total distance travelled of the mouse.

Fentanyl at 1 mg/kg promptly increased the total distance travelled in mice, and the effect was persistent up to 105 min. Increasing the doses, fentanyl (6 and 15 mg/kg) transiently reduced spontaneous locomotion up to 15 min, while it enhanced the motor activity in mice from about 45 to 165 min. The effects of fentanyl on spontaneous locomotion were no longer evident after 180 min and the mice motor activity was similar in fentanyl and vehicle-treated animals at 225 min (Figure 11C). To reveal a potential effect of fentanyl under these experimental conditions, we stimulated the motor activity of the mouse by means of a mechanical stimulus. Mechanical stimulation of the mouse promotes a transient but significant increase in the motor activity of the vehicle-treated animal at 225 min (Figure 11D) while the groups of animals treated with fentanyl showed a persistence of the inhibitory effect of the opioid on motor activation. In fact, mechanically stimulated motor activity was partially reduced in the group treated with fentanyl 1 mg/kg and totally prevented in those treated with fentanyl at 6 and 15mg/kg ($p < 0.05$; Figure 11D).

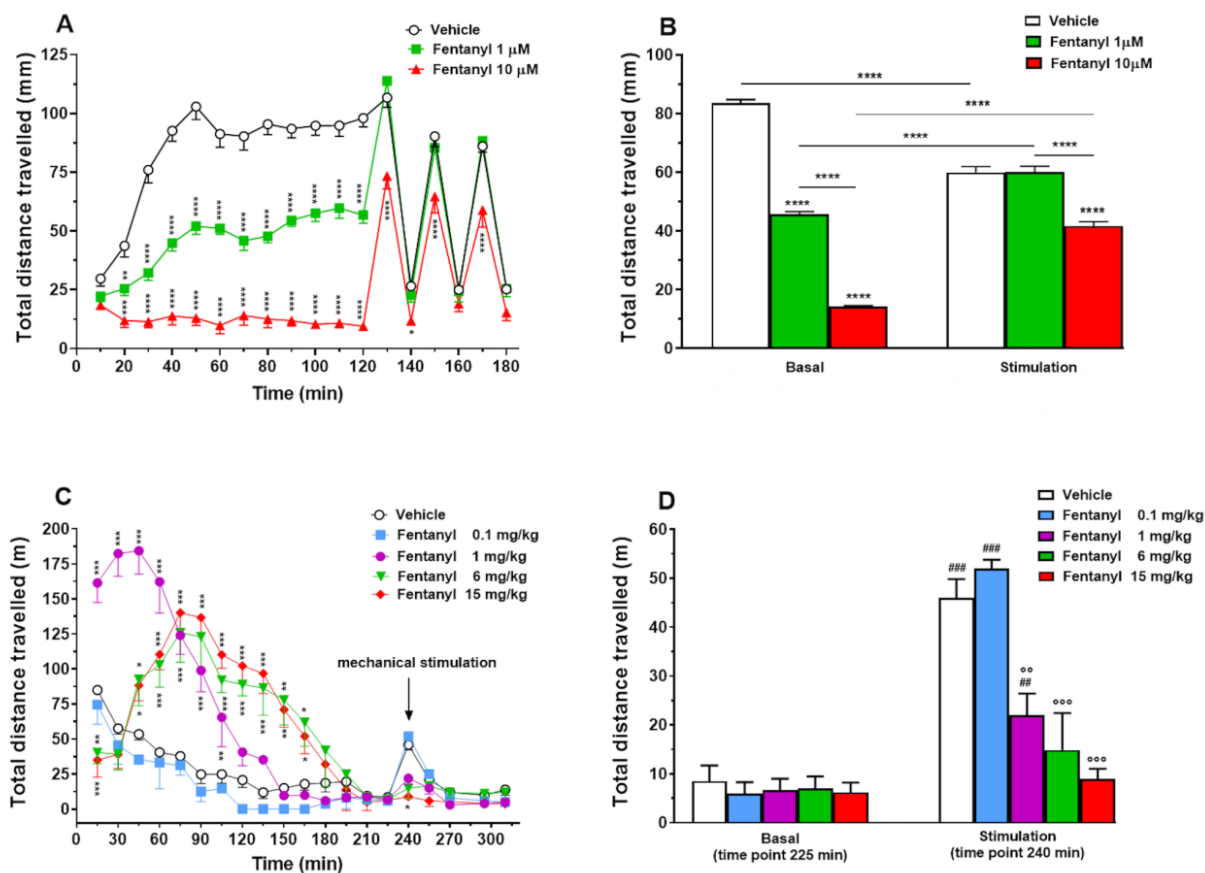


Figure 11: Behavioral test in zebrafish larvae (Panel A-B) and mice (Panel C-D). (A). * $p=0.0103$, ** $p=0.0011$, *** $p<0.01$ **** $p<0.0001$ (B) * $p=0.0259$, ** $p=0.0043$, *** $p=0.0002$, **** $p<0.0001$. (C-D) * $p<0.05$, ** $p<0.01$, *** $p<0.001$ versus vehicle.

5.2.3.3 Metabolic assay

In the present study, a tentative identification of fentanyl metabolites was also performed. The analysis was conducted using LC-HRMS acquiring in full-scan mode. An untargeted metabolomic method was used as a first screening approach, followed by a data-dependent MS/MS analysis of the most abundant peaks. Analytes were identified on the bases of accurate mass (± 5 ppm), retention times and MS/MS spectra. Subsequently, the proposed metabolic pathway was drawn taking in consideration the most common metabolic routes in zebrafish larvae or in mice. A list of the identified compounds and their identification data is summarized in table 1. The treatment with fentanyl produced in ZL and mice phase I and phase II metabolites, but the parent drug was still present in both models. The observed biotransformation included hydroxylation, N-oxidation and N-dealkylation with the

loss of phenethyl moiety. Neither in ZL nor in mice urine despropionylfentanyl was detected.

Compounds			Zebrafish Larvae (Extract)		Mice (Urine)	
Name	Chemical formula	Precursor ion	RT	Major products	RT	Major products
Fentanyl	C ₂₂ H ₂₈ N ₂ O	337.2269	8.4	188.1430	8.4	188.1431
				216.1384		216.1386
				281.1989		281.1996
				105.0702		105.0704
M1	C ₁₄ H ₂₀ N ₂ O	233.1648	6.8	84.0844	6.8	84.0845
				177.1425		177.1425
				150.0949		150.0945
				216.1382		216.1432
M2	C ₂₂ H ₂₈ N ₂ O ₂	353.2223	7.8	204.1373	7.8	n.d.
				121.0643		
				150.0906		
				162.0905		
M3	C ₂₂ H ₂₈ N ₂ O ₂	353.2223	8.8	186.1318	8.8	n.d.
				245.1698		
				105.0721		
				279.1819		
M4	C ₂₂ H ₂₈ N ₂ O ₂	353.2223	n.d.	n.d.	7.6	188.1495
						105.0762
						232.1417
						271.8863
M5	C ₂₂ H ₂₈ N ₂ O ₂	353.2223	8.6	245.1634	8.6	n.d.
				189.1372		
				146.0951		
				105.0691		
M2'	C ₂₈ H ₃₆ N ₂ O ₈	529.2544	7.2	353.2256	7.2	n.d.
				204.1397		
				121.0666		
				77.0385		
M3'	C ₂₈ H ₃₆ N ₂ O ₈	529.2544	7.5	335.2177	7.5	n.d.
				353.2283		
				279.1893		
				186.1354		
M4'	C ₂₈ H ₃₆ N ₂ O ₈	529.2544	n.d.	n.d.	7.4	353.2513
						188.1580
						105.0780
						233.1810

Table 1: List of metabolites tentative identified in zebrafish larvae and mice with the proposed fragmentation spectra. The metabolites are rated from + to ++++ according to their peak areas. (n.d.: not detected).

As depicted in figure 12, the major route of metabolism in ZL and mice is the N-dealkylation to norfentanyl, which represents the main metabolite detected in both the animal models. The second most represented metabolite in ZL was M2 obtained from the hydroxylation on the phenyl ring of the phenethyl moiety, whereas the other hydroxylated metabolite, β -hydroxyfentanyl (M3), was less abundant. Another minor metabolite detected was M5, obtained from the N-oxidation on the piperidine ring. As per phase II metabolites, only two conjugated forms of hydroxyfentanyl were detected in ZL (M2' and M3').

In mice urine, only norfentanyl and ω -1-hydroxyfentanyl (M4) and its conjugated form were found.

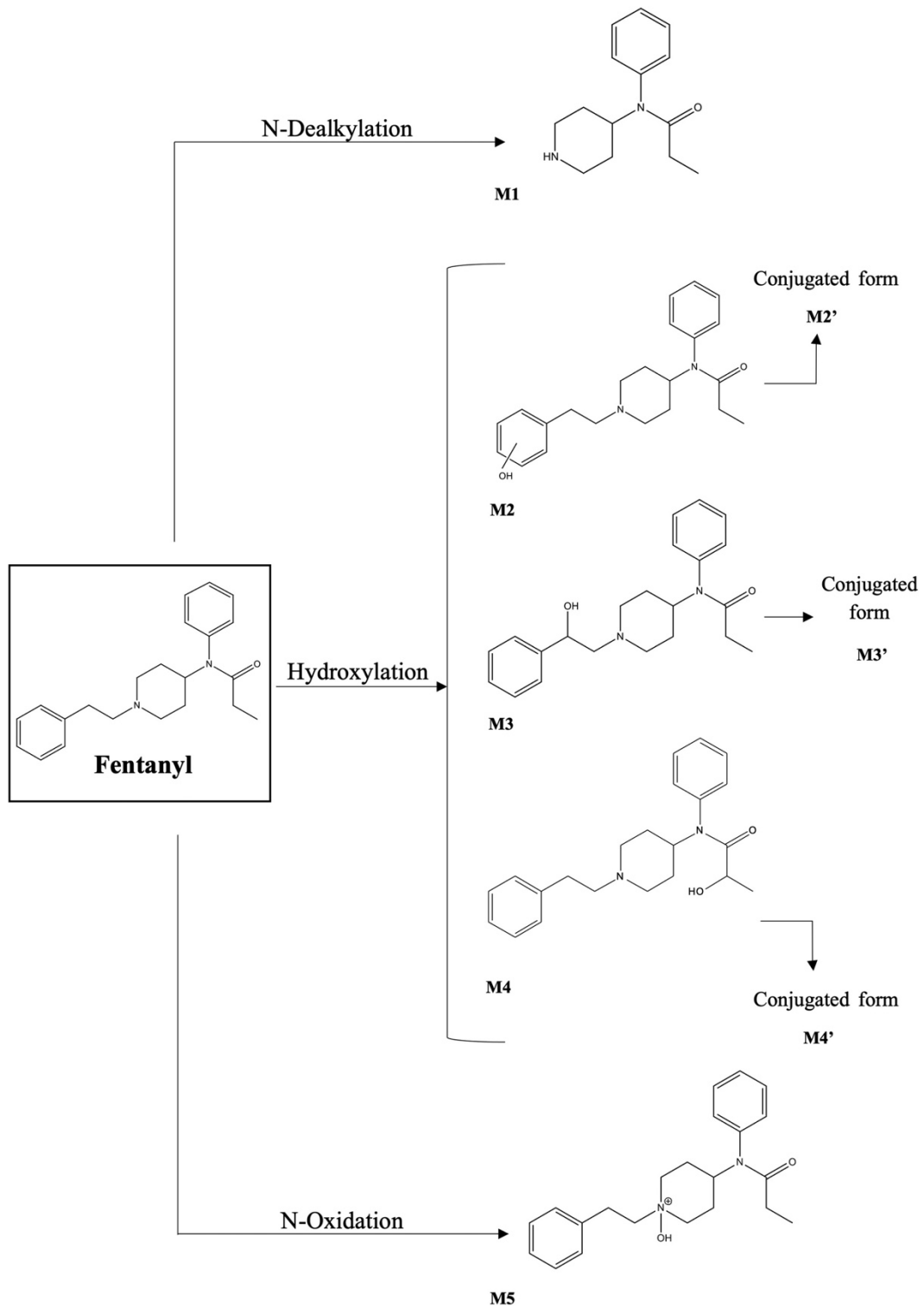


Figure 12: Schematic representation of proposed metabolic pathway of fentanyl, in mice (m) and zebrafish larvae (ZL).

5.2.4 Discussion

The behavioral effects of fentanyl and its derivatives on zebrafish are not fully established. However, it has been reported in two recent studies that acute

administration of fentanyl to zebrafish larvae (12–14 dpf) at the concentration of 1 μM did not affect the swimming velocity⁷³. Similar findings were observed in locomotion of adult zebrafish (4 weeks of age) at 0.3 μM ⁷⁴. At a first glance, these data do not fit with the present findings, but this could be justified with differences in fish age, concentrations of the drug used and applied methodologies. Moreover, the hypolocomotion observed in the basal phase (120 min) could be related to the sedative effect induced by fentanyl at 1 μM , considering that during the stimulated phase treated and untreated fish showed a similar travelled distance. Some previous studies have reported that opioids can increase locomotion⁷⁵ or induce biphasic effects⁷⁶. Since respiratory depression in zebrafish has been reported at the concentration of 1 μM , it could be hypothesized that respiratory alterations could affect the swimming activity of zebrafish and thus reduce locomotion⁷³. The zebrafish opioid system is more complex than that of vertebrates and humans due to the evolutionary differentiation of receptor sequences. Nevertheless, it shows similar pharmacological properties and conserved functions in respect to the mammals⁷⁷.

In the present study, in contrast to zebrafish, the rodent model showed hyperlocomotion induced by low doses (1 mg/kg) of fentanyl. These findings are in agreement with several studies, confirming that in rodents the facilitation of locomotion is triggered by the activation of the mesolimbic dopaminergic system, which is regulated by the endogenous opioid system, controlling the release of dopamine in the *nucleus accumbens*^{78–80}. Moreover, due to the affinity to serotonin receptors (5-HT1A)⁸¹, fentanyl could increase locomotion involving the opioid-serotonin system⁸². The mechanical stimulation did not affect animals treated with the range dose 1–15 mg/kg at 245 min (Figure 11 C and D). This effect could be related to the respiratory depression seen in mice^{63,83} and/or the muscle rigidity as reported in rats⁸⁴ and in cases of fentanyl users⁸⁵.

As regards the metabolic assay, previous studies carried out both *in vivo* and *in vitro* models^{86,87} showed that fentanyl is mainly metabolized to norfentanyl by N-dealkylation at the piperidine ring; only less than 1% is converted by alkyl hydroxylation or combined N-dealkylation and hydroxylation to hydroxyfentanyl and hydroxynorfentanyl. Fentanyl hydroxylation can occur on different positions,

mostly on the 2nd or 3rd position of the piperidine ring, at the ethyl linker of the phenethyl moiety, at the phenyl ring of the anilino moiety or the phenyl ring of the phenethyl moiety, or along the amide alkyl chain. Another minor metabolite described is despropionylfentanyl (4-ANPP), resulting from carboxamide hydrolysis of the fentanyl scaffold.

Our data in ZL were consistent with the results in mice urine. As a matter of fact, several metabolic pathways including N-dealkylation, hydroxylation at different positions and glucuronidation were observed in zebrafish. Generally speaking, considering that fentanyl and fentanyl analogs metabolism in human involves reactions like hydroxylation, N or O- dealkylation or O-methylation, the identified metabolic profile is consistent also with previously published studies on fentanyl metabolism in humans^{88,89}.

5.3 Study of toxicity and behavioral effects of ocfentanil and 2-furanylfentanyl in zebrafish larvae and mice

After the promising results obtained in the first year of my PhD, during my second year we deeply considered zebrafish as alternative animal model for toxicological studies. In this frame, we tried to test in zebrafish two fentanyl analogs, namely ocfentanil and 2-furanylfentanyl and we compared the results of behavioral and metabolic assay to those obtained in mice in collaboration with the Pharmacology Unit at the University of Ferrara.

5.3.1 Ocfentanil and 2-furanylfentanyl

Ocfentanil (N-(2-fluorophenyl)-2-methoxy-N-[1-(2-phenylethyl)piperidin-4-yl]acetamide) is a synthetic opioid structurally related to fentanyl, differing from it because of an extra fluorine atom on the *o*- position of the aniline moiety and a methoxy instead of a methyl group (see figure 12). It was first produced in the early 1990s with the aim of creating a potent naloxone-reversible opioid with less cardiovascular effects and respiratory depression. Ocfentanil (OcF) is sold in a white granular or brown powder, which is available either as free base or as hydrochloric acid salt⁹⁰. Ocfentanil potency is approximately 2.5 times higher than that of fentanyl⁹¹. Indeed, its assumption causes analgesia and respiratory depression in a dose-dependent manner, reaching the maximum peak after six minutes of the injection; analgesia disappears largely after one hour, while respiratory depression tends to last longer than fentanyl⁹². A study regarding dose-dependent pharmacological effects in humans was conducted by Fletcher *et al.* in 1991, however no conclusion about its benefits over fentanyl was drawn⁹³. To date ocfentanil has not been approved for any medical use.

Two-furanylfentanyl (N-phenyl-N-[1-(2-phenylethyl)piperidin-4-yl]furan-2-carboxamide) (or FuF) is a synthetic opioid with a structure similar to fentanyl, differing only in the replacement of the propionyl group with a furan ring (see figure 13)⁹⁴. The above-mentioned modifications grant sevenfold higher potency over fentanyl⁸⁸. FuF was first described in 1958 and, to date, has not yet been approved for any medical purpose^{95,96}. FuF has been available in the European Union since

June 2015, having been identified in 16 Member States and in Norway. In the United States this opioid appeared in December 2015. Several acute intoxications have been reported^{97,98} and in 2018 FuF was included in schedule I of the Controlled Substances Act^{94,99}. Fu-F is commonly sold as a powder but other forms such as liquid, tablets, or nasal spray are also available in the market¹⁰⁰.

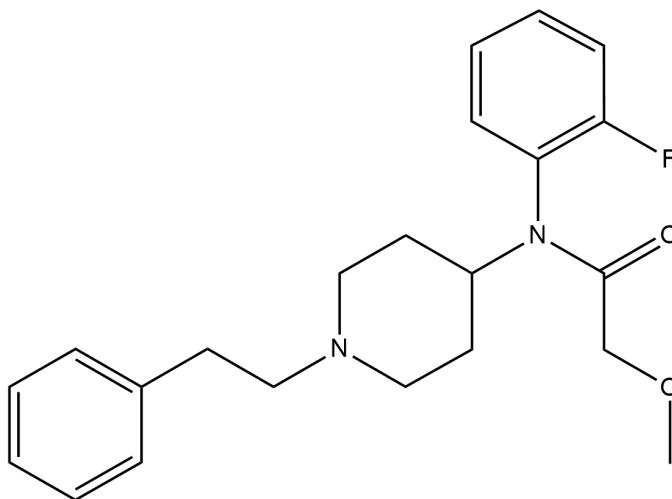


Figure 12: Oxycodone chemical structure.

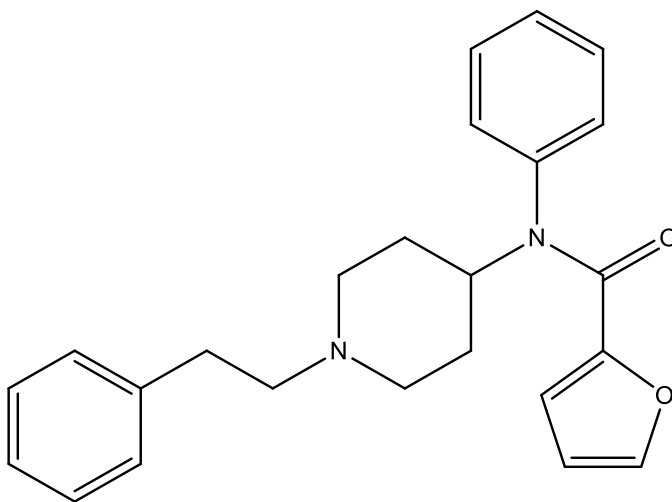


Figure 13: 2-furanylfentanyl chemical structure.

5.3.3 Materials and Methods

5.3.3.1 Morphological assay

The initial step involved a macroscopical evaluation of the morphological defects caused by ocfentanil and 2-furanylfentanyl (Comedical, Trento, Italy). For this purpose, a total of seventy zebrafish larvae underwent a 24 h-incubation at 28° C on the fourth day post fertilization. ZL were placed in 48-well plates with one larva per well and exposed at two concentration levels (1 and 10 µM). These concentrations were selected according to the previous study regarding the maximum tolerated concentrations of fentanyl in zebrafish. After 24 hours, larvae were anaesthetized by using ice and then monitored using a model DM2500 microscope connected with a model ICC50W camera.

5.3.3.1 Behavioral assay

Ocfentanil and 2-furanylfentanyl standards utilized for ZL behavioral assay were diluted in a solution of fish water medium; final tested doses were 1 and 10 µM.

Two replicates of each assay were performed on two different days. Overall, for behavioral tests 14 larvae (n= 7 for each replicate) were used for each dose. Moreover, in order to evaluate a potential solvent effect, control larvae were exposed to 0.3%, 3.3% methanol solution (vehicle 1 and 2, respectively) and to fish water. On the fourth day after fertilization, larvae were individually placed in 48-well plates filled with 1 ml of fish water medium and treatment, either ocfentanil, 2-furanylfentanyl or vehicle control, just before behavioral test.

Larvae were placed into the DanioVision tracking system as described in section 5.2.2.2. Also in this case, larvae were exposed for 120 minutes to white light for *habituation*, and then the *startle test* started with three successive light-to-dark transitions for a total test duration of 180 minutes. Experimental data obtained by the EthoVision software were split according to the two concentration levels i.e., 1 µM (0.33% methanol) and 10 µM (3.3% methanol) with the purpose of assessing the potential influence of the vehicle (water and methanol).

The same behavioral experiment performed for fentanyl was replicated for ocfentanil and 2-furanylfentanyl. A single mouse was placed in a square plastic and

changes induced by ocfentanil and 2-furanylfentanyl (LGC Standards S.r.l, Sesto San Giovanni, Milan, Italy) in motor activity were monitored for 310 min^{61,62} by means of an ANY-maze video-tracking system. Four mice were monitored at the same time in each experiment. At minute 225, each mouse was gently touched on its back three consecutive times with a plastic stick with a rounded tip. In the analysis of spontaneous locomotion in the open field test for each treatment (vehicles or 4 different 2-furanylfentanyl or ocfentanil doses, 0.1, 1, 6 and 15 mg/kg) 8 mice were used (total mice used: 80).

5.3.3.3 Metabolic assay

The instrument and the method used is the same above-described: a series 1260 HPLC in tandem with a 6540 Accurate-Mass QTOF. For details of the instrument and the method see section 5.2.2.3.

After the morphological assay, larvae were euthanized with ice. Afterwards, *treated* and *control* larvae were collected separately and snap-frozen at – 80° C and stored until the extraction performed as described above.

As regard mice, for each treatment (vehicle and 15 mg/kg 2-furanylfentanyl or ocfentanil) 8 mice were used (total mice used: 24). For the identification of metabolites, urines were collected after the injection of vehicle, 2-furanylfentanyl or ocfentanil at 15 mg/kg doses in a time interval of 0–5 h. Urine samples were kept at – 80° C until analysis. After dilution (1:1000) in autosampler vials with ultrapure water, samples were directly injected into the LC-QTOF.

5.3.3.4 Statistics

The statistical analysis was performed using GraphPad Prism software (Version 8). Normal response distributions were verified using Shapiro-Wilk normality test. Afterwards for ZL a two-way ANOVA test followed by a Dunnett's multiple comparison test were conducted to evaluate the effect over time of the two drugs at the lowest concentrations (1 µM). However, for the highest concentrations (10 µM) a two- way ANOVA and a Tukey post-hoc test were used. Moreover, Kruskal-Wallis and Dunn's tests were assessed to measure significant differences

($p < 0.0001$) between the three phases of the behavioral test compared to the vehicle (habituation, light off, light on).

To evaluate the effects of 2-furanylfentanyl or ocfentanil in mice at different doses over time compared to the vehicle, a two-way ANOVA followed by a Bonferroni test for multiple comparisons was performed. Furthermore, the comparison of the effects induced by 2-furanylfentanyl or ocfentanil on the response to mechanical stimulation of locomotion was conducted using a two-way ANOVA followed by a Bonferroni test for multiple comparisons. Finally, a Student's t-test was used to determine statistical significance ($p < 0.05$) between the different groups (see motor changes after mechanical stimulation).

5.3.4 Results

5.3.4.1 Morphological assay

In 2-furanylfentanyl-treated larvae, the concentration of $1 \mu\text{M}$ did not induce morphological changes in ZL. On the other hand, the highest concentration ($10 \mu\text{M}$) caused a yolk sac edema in 62.5% of cases, which is noticeable as a swollen abdomen in fig. 14. In addition, skin pigmentation in larvae treated with 2-furanylfentanyl was darker than the control larvae. On the contrary, ZL treated with ocfentanil at the two concentrations tested (1 and $10 \mu\text{M}$) did not show any malformations. On this basis, since at those concentrations, larvae did not seem to be suffering, it was decided to use these doses for further experiments.



Figure 14: Morphological effects on ZL.

5.3.4.2 Behavioral assay

Regarding ZL experiments, as depicted in figure 15 panel A, the statistical analysis showed a significant effect of treatment ($F_{2738}=444$, $p<0.0001$), time ($F_{17,738}=292.6$, $p<0.0001$) and time x treatment interaction ($F_{34,738}=34.38$, $p<0.0001$). Indeed, there was a significant decrement in larvae locomotion under the effect of the two synthetic opioids in the *habituation* phase (time point 120), whereas only 2-furanylfentanyl declined the movement during the *stimulation* phase (120–180 min). The above-mentioned effect was more pronounced at the highest concentration for 2-furanylfentanyl: in fig. 15 panel B, the two-way ANOVA showed a significant effect of treatment ($F_{2684}=5086$, $p<0.0001$), time ($F_{17,684}=40.23$, $p<0.0001$) and time x treatment interaction ($F_{34,684}=71.91$, $p<0.0001$). Overall, 2-furanylfentanyl dramatically inhibited the activity of ZL. As per the lowest drug concentration (1 μM), in the *habituation* phase both fentanyl analogs reduced the total distance travelled when compared to the vehicle. There was a significant increase in activity in the *light off*-phase compared to *habituation*, whereas movement in the *light on*-phase declined equally in treated and control larvae (Fig. 15; Panel C). Conversely, 2-furanylfentanyl at the highest concentrations (10 μM), reduced and flattened the total distance travelled overall, while ocfentanil 10 μM showed a decrease in locomotion compared to the vehicle only in the *habituation* phase (Fig. 15; Panel D). The bar chart was split in three different conditions namely *habituation*, *light off* and *light on*.

Spontaneous locomotion in mice was significantly affected by systemic administration of 2-furanylfentanyl (Fig. 16; Panel A: significant effect of treatment ($F_{4700}=31.27$, $p<0.0001$), time ($F_{19,700}=42.22$, $p<0.0001$) and time x treatment interaction ($F_{76,700}=7.118$, $p<0.0001$)) and ocfentanil (Fig. 16; Panel C: significant effect of treatment ($F_{4700}=58.98$, $p<0.0001$), time ($F_{19,700}=47.80$, $p<0.0001$) and time x treatment interaction ($F_{76,700}=9.917$, $p<0.0001$)) in the 0.1–15 mg/kg range of doses. Two-furanylfentanyl and ocfentanil at 1 mg/kg rapidly increased the total distance travelled in mice, and the effect lasted up to 90 min. By increasing the dose, both compounds at 6 mg/kg transiently reduced spontaneous locomotion at 30 min minutes after injection, while they enhanced locomotion from about 60 to 150–180 min. The opioid agonists at the highest dose (15 mg/kg) significantly

inhibited the total distance travelled in the first 30 min, while they facilitated locomotion up to 150 min (Fig. 16; Panel A and C). The effects of 2-furanylfentanyl and ocfentanil were no longer evident after 180 min and the spontaneous locomotion of mice was similar in 2-furanylfentanyl- ocfentanil- and vehicle-treated animals at 225 min (Fig. 16; Panel A and C).

Mechanical stimulation of the mouse promoted a transient but significant increase in the motor activity of the vehicle-treated animal at 225 min (Fig. 16; Panel B and D) while the groups of animals treated with 2-furanylfentanyl and ocfentanil showed a persistence of the inhibitory effect of the opioid on motor activation.

In fact, mechanically stimulated motor activity was completely reduced in the group treated with 1–15 mg/kg 2-furanylfentanyl ($F_{9,70}=11.73$; $p<0.0001$; Fig. 16; Panel B). Ocfentanil partially prevented (at 1 mg/kg) and completely reduced (at 6 and 15 mg/kg) the mechanically stimulated motor activity in mice ($F_{9,70}=19.22$; $p<0.0001$; Fig. 16; Panel D). The observed discrepancies between the two compounds at the dose of 1 mg/kg could be related to differences in their pharmacokinetics in response to various motor tests¹⁰¹.

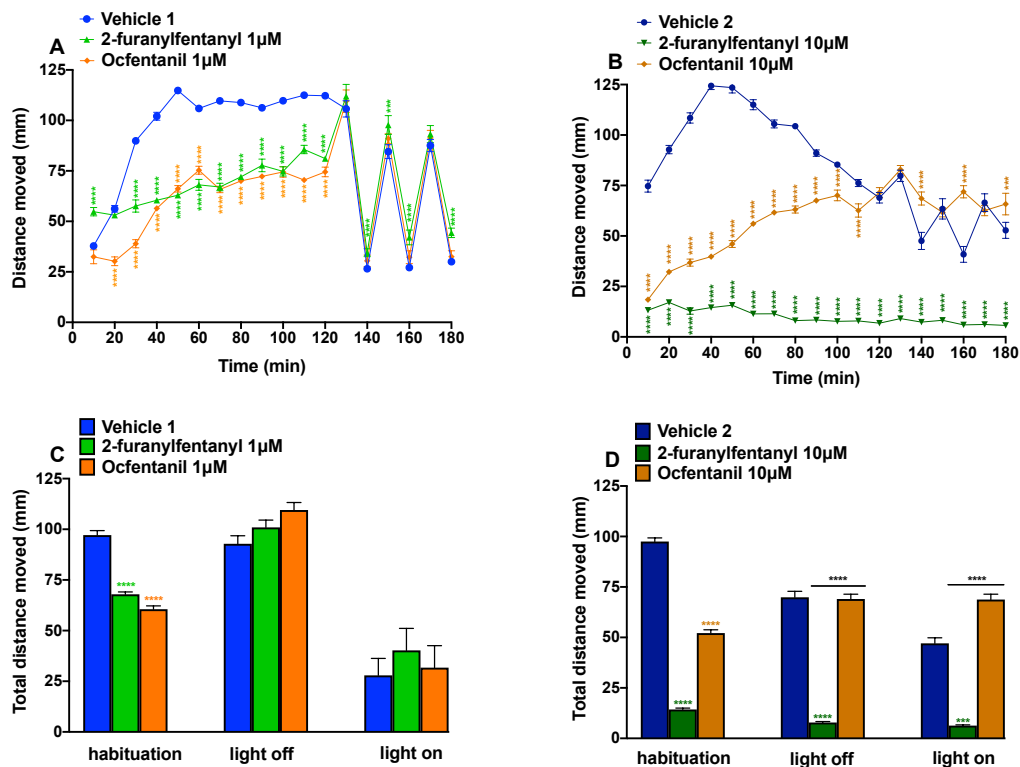


Figure 15: Behavioral assay on zebrafish larvae. Behavioral response to 2-furanylfentanyl and ocfentanil at the two-concentration level of 1 μM (Panel A, C) and 10 μM (Panel B, D) in ZL. Vehicle 1 and 2 consisted of fish water containing 0.3% and 3.3% of methanol, respectively. Data are expressed as the mean ± SEM of the total distance travelled. *** $p<0.001$, **** $p<0.0001$.

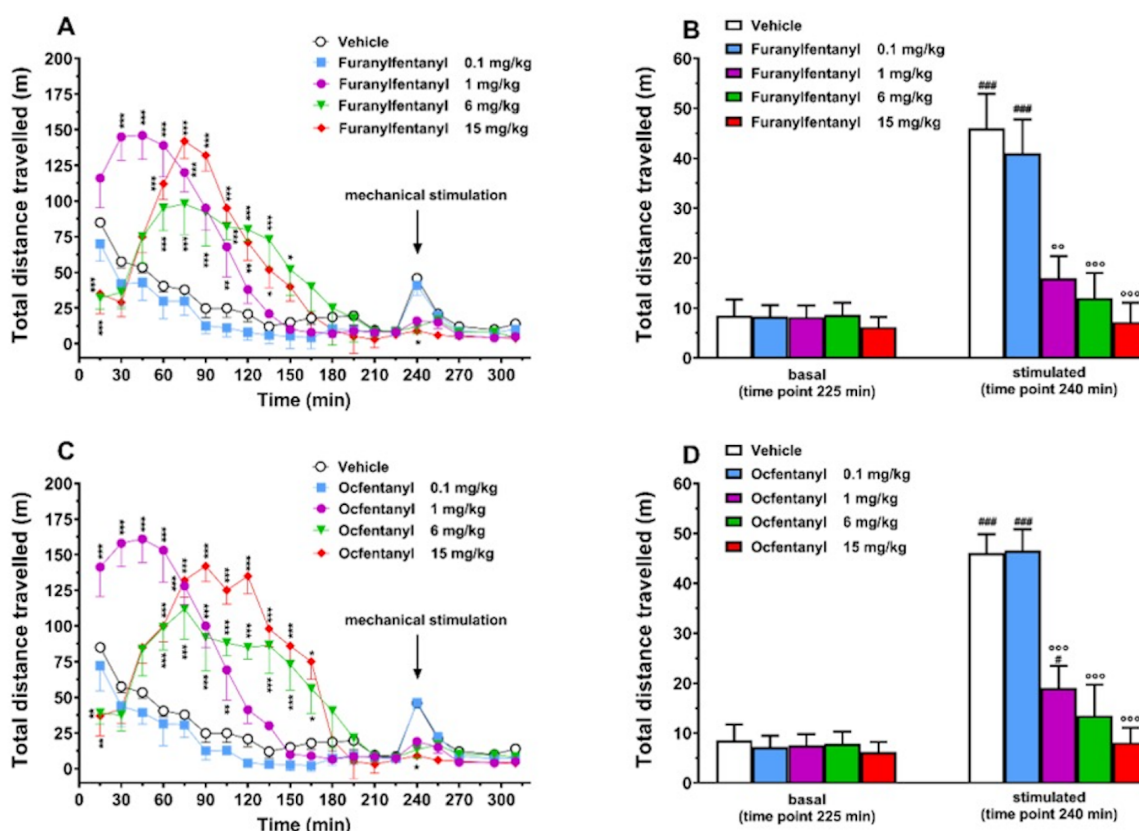


Figure 16: Behavioral assay on mice. Effect of the systemic administration of 2-furanylfentanyl (0.1–15 mg/kg i.p.; Panel A, B) and ocfentanil (0.1–15 mg/kg i.p.; Panel C, D) on the total distance travelled by the mouse. * $p < 0.05$, ** $p < 0.01$, *** $p < 0.001$ versus vehicle; # $p < 0.05$, ### $p < 0.001$ versus basal; ° $p < 0.01$, °° $p < 0.001$ versus stimulated responses.

5.3.4.3 Metabolic assay

The analysis of 2-furanylfentanyl and ocfentanil metabolites was conducted using LC-HRMS acquiring data in full-scan mode. The identification of metabolites was performed by considering accurate mass (± 5 ppm), retention times and MS/MS spectra.

The current study identified a total of six metabolites of 2-furanylfentanyl (Table 2). The corresponding metabolic pathway is shown in fig. 17. On the bases of the relative amount of peak area, in larvae extracts the main metabolites were nor-furanylfentanyl (M1) and hydroxy-furanylfentanyl (M2), resulting from the hydroxylation on the phenethyl group and the corresponding conjugated form (M2'). Other minor metabolites detected were M3, obtained from N-oxidation on the piperidine ring, hydroxy-methoxyfuranylfentanyl (M4) and dihydrodiol

metabolite (M5), resulting from hydration on the furan ring. In contrast with ZL, only dihydrodiol metabolite and M2' were identified in mice urine.

On the other hand, seven ofentanal metabolites were detected in the two animal models, resulting from hydroxylation or/and demethylation of the parent drug (Table 3). The mono-hydroxylation occurred in three different positions in larvae, i.e., at the phenyl ring of the phenethyl moiety (M1), in β -position of the ethyl linker (M2) and at the piperidine ring (M3). On the contrary, in mice urine only M4, resulting from hydroxylation in ω -position, was detected. O-desmethyl ofentanal (M5), corresponding to the loss of methyl of the methoxy group, was also identified in zebrafish larvae as well as in mice urine, representing in the latter the most abundant metabolite along with its conjugated form (M5'). Another hydroxylation occurred in ZL at the fluorophenyl moiety of M5, forming M6 (hydroxy-O-desmethyl-ofentanal) (Fig. 18). Strangely enough, two of the most common biotransformations described in fentanyl and in fentanyl analogs, namely N-dealkylation and the formation of 4-ANPP (flouro-despropionylfentanyl), were not detected in the two *in vivo* models tested.

Compound			Zebrafish Larvae (Extract)			Mice (Urine)		
Name	Chemical formula	Precursor ion	RT	Major products	%	RT	Major products	%
2-furanyl fentanyl	C ₂₄ H ₂₆ N ₂ O ₂	375.2068	8.6	188.1558 105.0703	+++	8.6	188.1467 105.0722	+++
M1	C ₁₆ H ₁₈ N ₂ O ₂	271.1384	7.0	188.0633 170.1110	++		n.d.	
M2	C ₂₄ H ₂₆ N ₂ O ₃	391.2016	7.9	204.1391 121.0653	++		n.d.	
M3	C ₂₄ H ₂₆ N ₂ O ₃	391.2016	8.7	105.0681 283.1390	+		n.d.	
M4	C ₂₅ H ₂₉ N ₂ O ₄	421.2122	7.9	234.1485 151.0754	+		n.d.	
M5	C ₂₄ H ₂₈ N ₂ O ₄	409.2124	7.9	188.1380 105.0653	+	8.0	188.1438 105.0701	+++
M2'	C ₃₀ H ₂₄ N ₂ O ₉	567.2337	7.4	391.1900 204.1320	++	7.5	391.1649 204.1181	++

Table 2: List of metabolites tentative identified in zebrafish larvae and mice treated with 2-furanylfentanyl. The metabolites are rated from + to ++++ according to their peak areas. (n.d.: not detected).

Compound			Zebrafish Larvae (Extract)			Mice (Urine)		
<i>Name</i>	<i>Chemical formula</i>	<i>Precursor ion</i>	<i>RT</i>	<i>Major products</i>	<i>%</i>	<i>RT</i>	<i>Major products</i>	<i>%</i>
Ocfentanil	C ₂₂ H ₂₇ FN ₂ O ₂	371.2135	7.9	188.1504 105.0697	+++	7.9	188.1426 105.0694	+++
M1	C ₂₂ H ₂₇ FN ₂ O ₃	387.2084	7.2	204.1470 121.0700	++		n.d.	
M2	C ₂₂ H ₂₇ FN ₂ O ₃	387.2084	8.2	279.1510 105.0697	++		n.d.	
M3	C ₂₂ H ₂₇ FN ₂ O ₃	387.2084	7.5	204.1294 186.1181	+		n.d.	
M4	C ₂₂ H ₂₇ FN ₂ O ₃	387.2084		n.d.		8.7	371.2512 89.0641	+
M5	C ₂₁ H ₂₅ FN ₂ O ₂	357.1978	7.6	188.1459 105.0703	++	7.6	188.1443 105.0706	+++
M6	C ₂₁ H ₂₅ FN ₂ O ₃	373.21020	7.9	189.1416 105.0672	+++		n.d.	
M5'	C ₂₇ H ₃₃ FN ₂ O ₈	533.2299		n.d.		7.2	357.2093 188.1499	++++

Table 3: List of metabolites tentative identified in zebrafish larvae and mice treated with ocfentanil. The metabolites are rated from + to ++++ according to their peak areas. (n.d.: not detected)

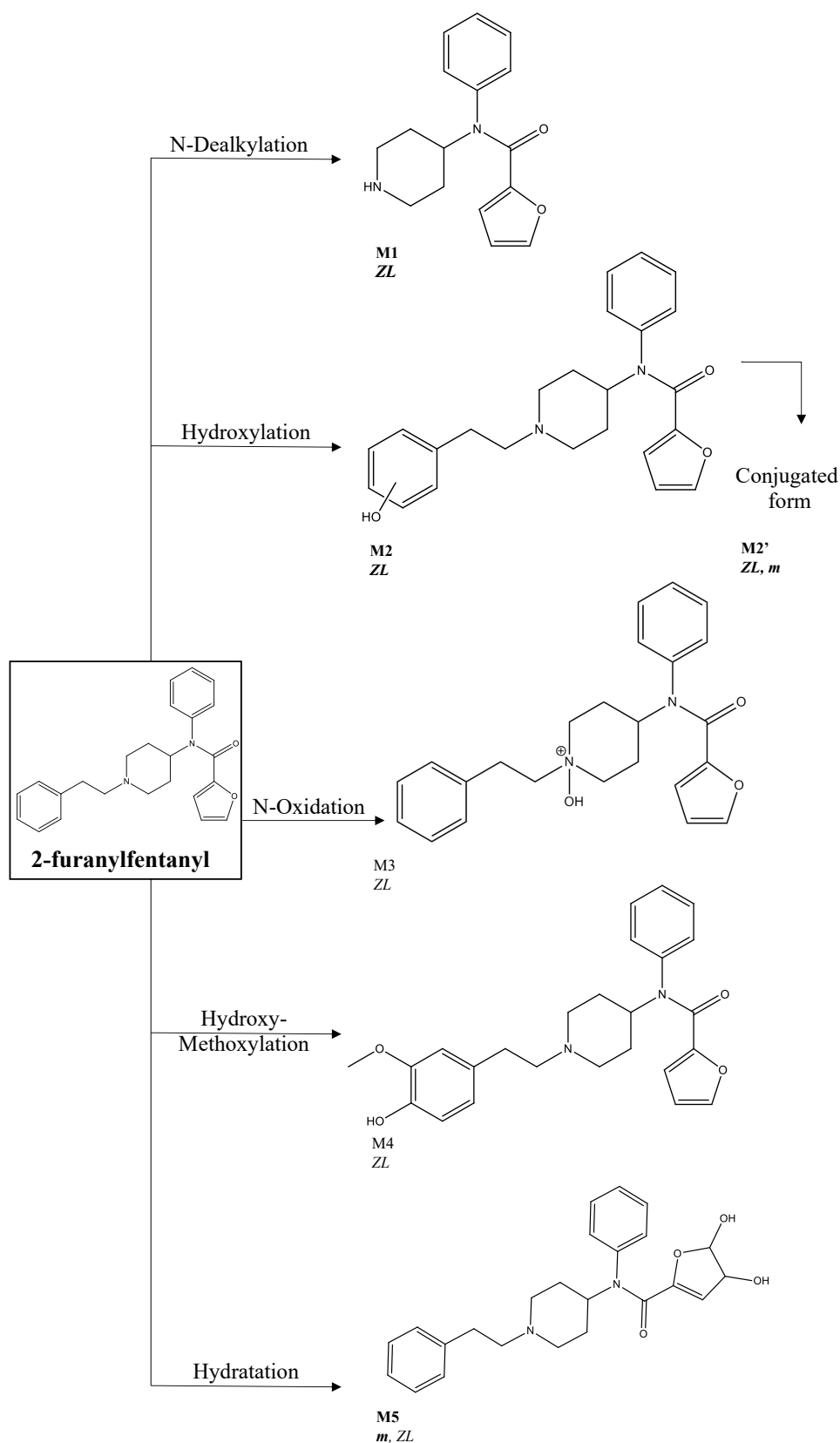


Figure 17: Two-furanylfentanyl metabolism. Schematic representation of proposed metabolic pathway of 2-furanylfentanyl, in mice (*m*) and zebrafish larvae (*ZL*). The main metabolic reactions and the resulting metabolites are highlighted in bold.

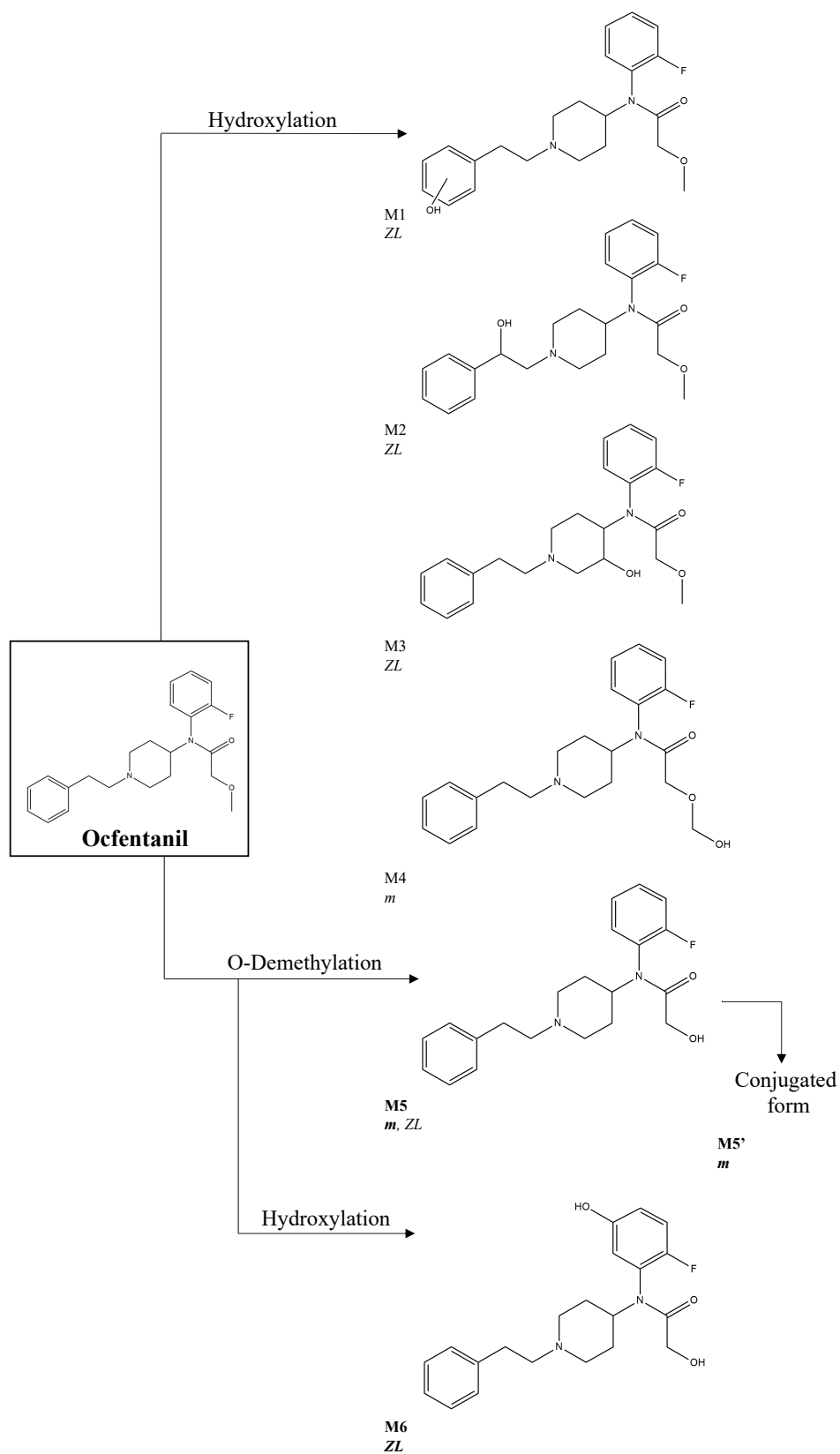


Figure 18: Ocfentanil metabolism. Schematic representation of proposed metabolic pathway of ocfentanil, in mice (*m*) and zebrafish larvae (ZL). The main metabolic reactions and the resulting metabolites are highlighted in bold.

5.3.5 Discussion

Overall, larvae locomotor activity was impaired after the treatment with the two opioids in both *habituation* and *stimulation* phases. In particular, at the lowest concentration (1 μ M), both 2-furanylfentanyl and ocfentanil decreased the locomotor activity of ZL. A significant dose-dependent reduction in activity due to fentanyl and fentanyl analogs at a comparable concentration was also recently reported in a similar behavioral study in ZL⁶⁶.

In this thesis, it was also demonstrated that a high concentration (10 μ M) of 2-furanylfentanyl and ocfentanil induced an inhibitory locomotor effect in ZL in habituation, light on and light-off phases. Moreover, the vehicle used for higher concentration induced a slight increase of the locomotion in ZL. This effect could be related to an enhancement of the direct toxicity exerted by the two compounds¹⁰² or may also be caused by the synergic effect of methanol present in the vehicle. To investigate the possible role of methanol, a specific study was performed. The influence of methanol on the locomotor activity in ZL was evaluated by incubating larvae with fish water containing 0, 0.3% and 3.3% methanol. Larvae seem not to be sensitive to methanol, except for a slight effect observed with methanol at 3.3%. However, the inhibition of locomotor activity exerted by ocfentanil and 2-furanylfentanyl at the concentration of 10 μ M observed in figure 15 panel B is higher than that related to the presence of methanol.

In ZL the effect of 2-furanylfentanyl was more significant than that induced by ocfentanil, but similar to the effect of fentanyl at the same concentration. These differences could be related to a higher toxicity of 2-furanylfentanyl compared to ocfentanil, at least at high doses. In fact, in the morphological test, 2-furanylfentanyl induced malformation in ZL at the dose of 10 μ M. In particular, the administration of this drug produced abdominal swelling, which has been reported as a common sign of acute toxicity in zebrafish⁶⁷. Moreover, it is known that the yolk sac lipophilicity provides an ideal compartment for the accumulation of hydrophobic toxicants¹⁰³. Therefore, the higher hydrophobicity of 2-furanylfentanyl could increase the accumulation of this drug in the yolk sac, causing the observed morphological toxicity. On the contrary, no alterations were observed

after incubation with ocfentanil or in fish water containing methanol. A further explanation could be that the malformations occurring after the administration of 2-furanylfentanyl 10 μ M, could create by itself a motor impairment, hence giving hypolocomotion in the behavior assay.

The administration of 2-furanylfentanyl and ocfentanil in mice (0.1–15 mg/kg) induced a significant impairment in motor activity, in particular at the dose of 1 mg/kg. These data are in accordance with the recent study of Varshneya¹⁰⁴ reporting the effect of ocfentanil.

Opioid receptor expression and activation in zebrafish have been demonstrated to be both biologically and pharmacologically comparable to that of rodents and humans^{105,106}. Furthermore, zebrafish opioid receptor transcripts could be detected in early development stages (before 3 h post fertilization). In the previous study, we demonstrated that, in contrast to zebrafish, the rodent model showed hyperlocomotion induced by low doses (1 mg/kg) of fentanyl. Our results confirm previous findings concerning differences in locomotor effects induced by opioids between the two models. In ZL the effect seems to be mediated by the activation of the mu opioid receptor, as highlighted by Zaig *et al.*⁷³. Different factors can account for these differences. For instance, an important element to be considered in the comparison between behavioral effects in ZL and mice is developmental stage. Indeed, reduced swimming activity in ZL treated with fentanyl analogues could be related to a higher sensitivity of embryos to toxicants compared with adult mice¹⁰⁷. In addition, zebrafish hypomotility could be related to earlier respiratory depression compared to mice at low concentrations of fentanyl and its analogs. In particular, differently from mammals, ZL have a complex respiratory system, which they use to move water through their gills for oxygen absorption and carbon dioxide elimination. Furthermore, differences in locomotor effects induced by 2-furanylfentanyl and ocfentanil between the two animal models could be related to differences in metabolism, as discussed below. Moreover, Zaig and his colleagues revealed that fentanyl induced respiratory depression in ZL, and this effect was reversed by a high concentration (20 μ M) of the mu opioid receptor antagonist naloxone⁷³.

According to the metabolic assay performed with the same animal models for fentanyl, ZL and mice showed relatively similar metabolic pathways. In particular, the analysis of larvae extracts identified a large number of phase I metabolites, mostly due to hydroxylation, hydration and oxidation, for 2-furanylfentanyl. On the contrary, mice mainly seemed to produce the dihydrodiol metabolite. The major route of metabolism for ocfentanil in ZL was hydroxylation, while in mice it was o-demethylation. The two models produced phase II metabolites, i.e., glucuronide metabolites. These results are partially consistent with previous studies on 2-furanylfentanyl metabolism in different experimental models (i.e. microsomes and human urine), where the major route of metabolism was represented by hydroxylation and formation of dihydrodiol metabolite^{94,95,108,109}. However, no 4-anilino-N-phenethylpiperidine (4-ANPP) was observed, pointing out that this common metabolite of fentanyl is not present in its analog. This difference might be due to a lack of the amidase enzyme involved in the production of 4-ANPP in ZL and in mice¹⁰⁹. On the contrary, ocfentanil results in mice and ZL are consistent with the metabolic pathway proposed by Allibe *et al.*¹¹⁰ in which the major route of metabolism *in vitro* and in biological samples was represented by hydroxylation, demethylation and glucuronidation, whereas 4-ANPP was not described and nor-ocfentanil was elucidated only in human liver microsomes, but not in biological samples. Our results confirm the validity of ZL for the identification of NSOs metabolites, even though they showed small differences in metabolism when compared to mice, which could be related to the different route of exposure as suggested for other opioids⁶⁶.

5.4 Study of metabolism and potential toxicity of nine synthetic opioid analogs using the zebrafish larvae model

The last step of my thesis project was focused on the possible application of zebrafish as actual screening tool for n=9 new synthetic opioid (see figure 19). Two of the tested compounds belong to the cinnamylpiperazine class (AP-237 and 2-methyl-AP-237), while seven to the 2-benzylbenzimidazole group (isotonitazene, metonitazene, etodesnitazene, N-pyrrolidino etonitazene, butonitazene, flunitazene and metodesnitazene). For the majority of these compounds, no or low data are present in literature, especially regarding the metabolic fate, which result in the lack of possible analytical target to be search in human fluids. Along with this aspect, an *in vivo* toxicity assay was performed, in order to test the apoptosis rate of each compound.

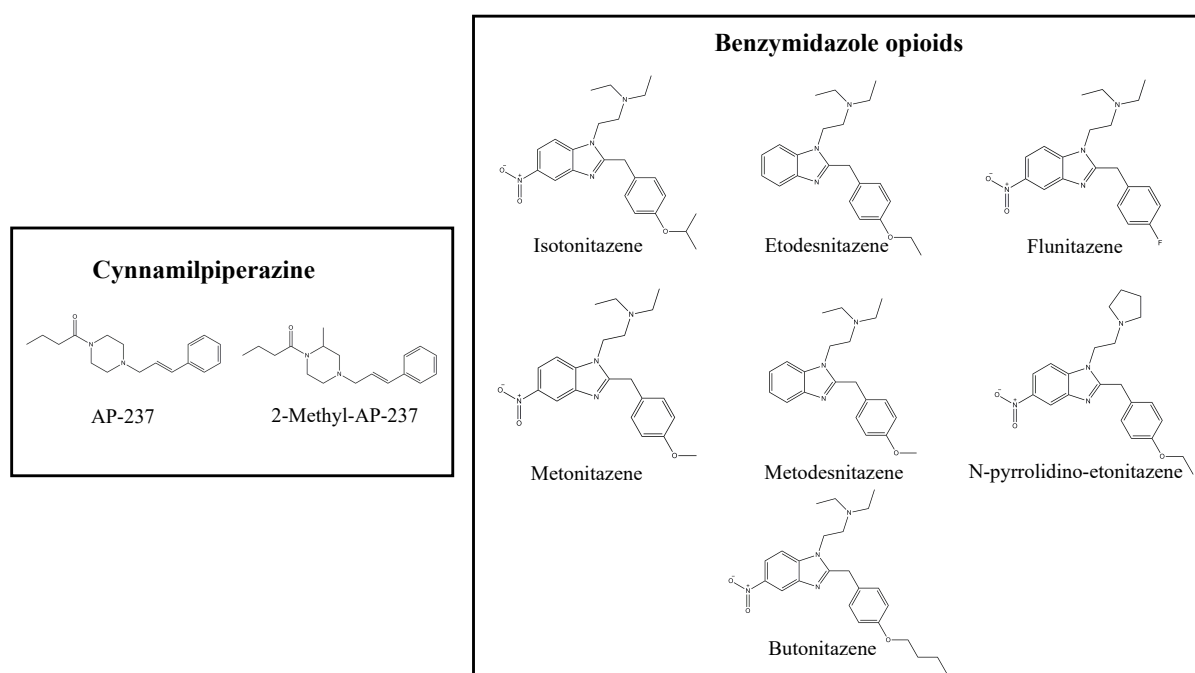


Figure 19: Molecular structures of the studied synthetic opioids.

5.4.1 Cinnamylpiperazine

Cinnamylpiperazines differ structurally from fentanyl analogs, which are characterized by a piperidine core and a phenethyl chain, for the presence of a piperazine ring and a cinnamyl moiety. Among cinnamylpiperazines, 2-methyl-AP-

237 (known also as 2-methyl bucinnazine) was the first detected for recreational purposes in 2019 in Slovenia¹¹¹. Structurally related to the former, AP-237 (Bucinnazine) was the second cinnamylpiperazine reported in the U.S.A¹¹². It was originally developed in Japan in 1968 as analgesic, showing a higher therapeutic index and less addictive nature than morphine¹¹³. For this reason, it is currently used for the treatment of cancer pain in China. Despite its clinical use in China, it is not authorized for any medical purposes in Europe or in the United States. The two compounds are often sold in *dark web* as “synthetic heroin” and since September 2020 the online mentions of these two compounds have seen a dramatic growth with a significant increase of deaths correlated to their use¹¹⁴.

5.4.2 Benzylbenzimidazole

Benzylbenzimidazole opioids were developed in the late 1950s-1970s by CIBA Aktiengesellschaft in Switzerland. Nevertheless, their appearance in the illicit market is very recent, sold not only in a pure form as powders or nasal sprays but also as components of counterfeit medicines or fortifiers for heroin, posing a risk for unaware customers^{115,116}. In the last years, this class of NPS has been associated with a number of fatalities in several countries, particularly in the USA¹¹⁷.

Isotonitazene is a strong opioid-based compound, structurally not related to fentanyl, known to be a full μ -opioid receptor agonist, with a potency estimated in a range between 100-1000 times as morphine, and no established medical use^{118,119}. First reported in 2019 in the USA, by October 2020 it has been the cause of death of more than 200 individual cases. In June 2020 it was inserted in Schedule I of the 1961 Convention by US Drug Enforcement Administration. Isotonitazene breakout started a surge of *nitazene analogs* on the recreational drug market and several other analogs were identified in toxicological samples, such as metonitazene.

Although it was firstly reported in 2020 in the United States, metonitazene was originally synthesized in 1957. Since August 2023, it has been officially included in Schedule I of Controlled Substances. Its potency was evaluated throughout an *in vitro* study, which reported a potency similar to that of fentanyl¹²⁰.

Etodesnitazene (known also as etazene), firstly detected in 2022, has an analgesic activity 70 times higher than morphine, however it is not approved for medical use.

Vandeputte and colleagues reported a high potency of the drug in the interaction with μ -opioid receptors ($EC_{50}=54.9$ nM), being a full agonist¹²⁰. Its chemical structure differs from the other benzimidazole derivatives due to the lack of a nitro group on the benzimidazole ring¹²¹. In July 2022, it was added by the WHO in a list of NPS to be considered for a critical review.

A novel member of benzoimidazole group is N-pyrrolidino etonitazene (etonitazepyne), which arises from etonitazene; however, in the new compound the two ethyl chains in the dimethylamine group are cyclized forming a pyrrolidine. It was chemically characterized and identified in a study of Blanckert *et al.* for the first time in a yellow powder sample purchased online by Belgian Warning System¹²². In February 2021, it was formally reported to EMCDDA Early Warning System (EWS). Furthermore, in a period between January and April 2021, the compound was identified in eight post-mortem cases. A study of Vandeputte and colleagues shows that N-pyrrolidino etonitazene is a selective and extremely potent MOR agonist, specifically 800 times more potent than morphine and roughly 40 times more potent than fentanyl¹²³.

Butonitazene was reported in Ohio alongside metonitazene in January 2021 but currently is not officially scheduled in the United State. Low data are present in the literature, mostly regarding its involvement in post-mortem cases^{119,124} or some potency assay¹²⁵. In this study, probably also due to its long alkoxy side chain, it is considered one of the least potent ($EC_{50} = 0.5$ nM).

Flunitazene was firstly reported in March 2020 and, as suggested by the name, it presents a typical fluorobenzyl structure. Its potency was studied by Vandeputte *et al.*¹²⁰, and considered one of the lesser potent nitazene analogs.

As for etodesnitazene, metodesnitazene lacks a nitro group on the benzimidazole ring. It was firstly reported in July 2021 in Ohio. Its potency seems to be equipotent with flunitazene and based on *in vitro* studies (as other nitazene analogs like butonitazene and metonitazene), data showed that it binds to and activates the μ -opioid receptor, and thus activating the β -arrestin-2. This interaction has been implicated in adverse health effects of many opioid analgesics, such as a high potential for addiction¹²⁶.

5.4.3 Materials and Methods

5.4.3.1 *In vivo cell death assay*

The presence of cellular toxicity was assessed *in vivo* on zebrafish samples by acridine orange (AO) staining (Sigma Aldrich, St. Louis, USA), a nucleic acid intercalant able to emit green fluorescence when bound to double-strand DNA and therefore used to estimate genome damage. Embryos - starting from 24 hours post fertilization - were treated with FW containing phenylthiourea (PTU) (Sigma Aldrich, St. Louis, USA) in order to reduce pigmentation. At the 4th day post fertilization, ten zebrafish larvae for each experimental condition were exposed for 24 hours to the tested drugs (at individual concentrations of 0.1 μ M) and then incubated with 5 μ g/mL of AO for 30 minutes at 28.5° C. Finally, larvae were washed 3 times with FW medium and mounted in 2% methylcellulose (Sigma Aldrich, St. Louis, USA). The acquisition of fluorescence was done with a model MZ 16 F microscope (Leica Microsystem Vertrieb GmbH, Wetzlar, German) and the presence of positive dots was assessed selecting a specific ROI (region of interest), including the head and the trunk until the end of the yolk extension, and then quantified by counting the fluorescent dots. Grubb's test was used for the detection of outliers which were excluded from the analysis. Differences between control and treated zebrafish were evaluated by Mann-Whitney test. Data are reported as mean \pm standard error of the mean (SEM) and the statistical significance threshold was set at $p < 0.05$.

5.4.3.2 *Morphological assay*

In order to evaluate possible morphological defects related to the studied opioids, each one of the 4th day-post-fertilization larvae was placed in a well of 48-well plates and exposed for 24 hours to 1 μ M of AP-237, 2-methyl-AP-237, isotonitazene, metonitazene, etodesnitazene, butonitazene, flunitazene, metodesnitazene and N-pyrrolidino etonitazene (Comedical, Trento, Italy). Control larvae were exposed to vehicle (3.3% methanol in FW). A total number of 150 larvae were monitored using a model DM2500 microscope connected with a ICC50W camera (Leica Microsystem Vertrieb GmbH, Wetzlar, German). Larvae were evaluated for several developmental malformations, including yolk sac and

pericardial edema, body axis, trunk length, caudal fin, pectoral fin, pigmentation, jaw and somite deformities according to the abnormalities highlighted by Noyes⁶⁰ and also elucidated in larvae exposed to increasing concentrations of fentanyl and fentanyl analogs in the first part of the project.

5.4.3.3 Metabolic assay

After the morphological evaluation, fifteen zebrafish larvae for each tested drugs (exposure for 24 hours to 1 μ M concentration) were euthanized in ice. The extraction of larvae was performed - as above - following the method developed by Gampfer's⁶⁴.

Analyses were carried out on a Vanquish UPLC coupled with an Orbitrap FusionTM LumosTM TribridTM Mass Spectrometer (Thermo Fisher Scientific, Whaltman, USA). This was only recently purchased by Centro Piattaforme Tecnologiche facility of the University of Verona and then used by us in the last part of the project for the advantages it offers, such as a high sensitivity and high resolution which makes it a powerful instrument for the identification and quantitation of small molecules.

A gradient chromatographic separation was performed on a Hypersil GOLD column (150x2.1 mm, 1.9 μ m particle size, Thermo Fisher Scientific, Whaltman, USA) thermostated at 35°C. A sample volume of 1 μ L was injected. The composition of the mobile phase was as follows: formic acid 0.1% as phase A and acetonitrile added with 0.1% formic acid as phase B. The gradient elution profile was: 0–0.5 min 5% B, 0.5–10.5 min linear gradient from 5 to 75% B, 10.5–11.5 min from 75 to 95% of B, 11.5-18 min hold 95%, 18-25 min hold 5% B. The flow rate was set at 280 μ L/min.

The heated-ESI ion source operated in positive (3300 V) and in negative (-3200 V) ionization mode. The ion source parameters were: vaporizer temperature, 300°C; sheath gas, 38 arbitrary unit (AU); aux gas, 10 AU; ion transfer tube temperature, 280°C.

An untargeted acquisition was performed as screening approach, followed by a data-dependent MS/MS analysis of the most abundant peaks. The settings for the full-scan data acquisition parameters were as follows: resolution, 60,000; scan

range, 100-1200 m/z. The setting for MS/MS experiments was as follows: resolution, 15,000; isolation window, 1.5 m/z. Fragmentation on the ions of interest was obtained by applying three different collision energy, 20, 40 and 80 eV. Analytes were identified on the bases of accurate mass (± 5 ppm), retention times and MS/MS spectra.

Compound related components were detected by comparison of extracted ion chromatograms of predicted mass transitions with a blank sample (i.e., untreated zebrafish larvae) or by using an untargeted approach. Metabolite structures of the hypothetical candidate were assigned on the basis of MS/MS structural assignment and accurate mass formulae prediction.

The acquisition software was Xcalibur version 3.4 (Thermo Fisher Scientific, USA).

5.4.4 Results

5.4.4.1 *In vivo cell death assay*

In this study, the *in vivo* acridine orange staining has been used to visualize events in embryos treated with the compounds under study.

As shown in figure 20, acridine orange staining was evident in all the embryos, especially in the eye, heart and swim bladder areas, as scattered spots of dead cells. As an example, in figure 20, control and larvae treated with metonitazene and butonitazene, after incubation with AO, are depicted. It is noteworthy that larvae treated with metonitazene showed a higher number of scattered spots compared with those exposed to butonitazene, especially in the heart region (highlighted with the arrow).

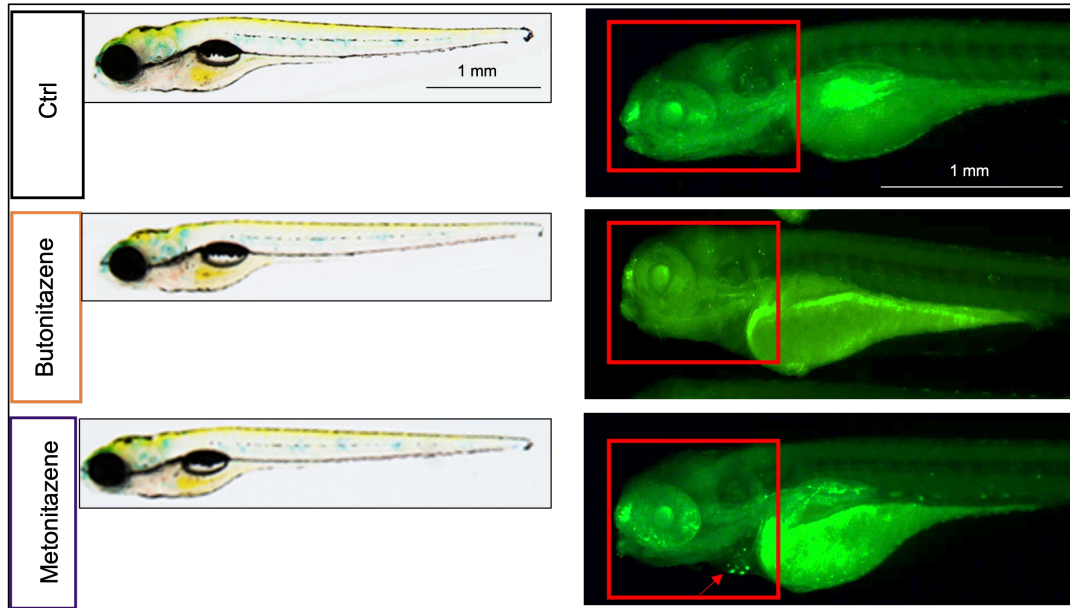


Figure 20: Cell death evaluation in 5 dpf exposed zebrafish larvae. Representative images of 5 dpf larvae untreated or treated with 0.1 $\mu\text{mol/L}$ of butonitazene and metonitazene: the arrow in figure indicates the heart region – full of green dot. The bright field picture confirmed the healthiness state of each larva.

The quantitative analysis (Figure 21) revealed that embryos treated with low dosages of synthetic opioids (0.1 μM) are characterized by a stronger acridine orange staining than the controls suggesting a cytotoxic effect of these compounds.

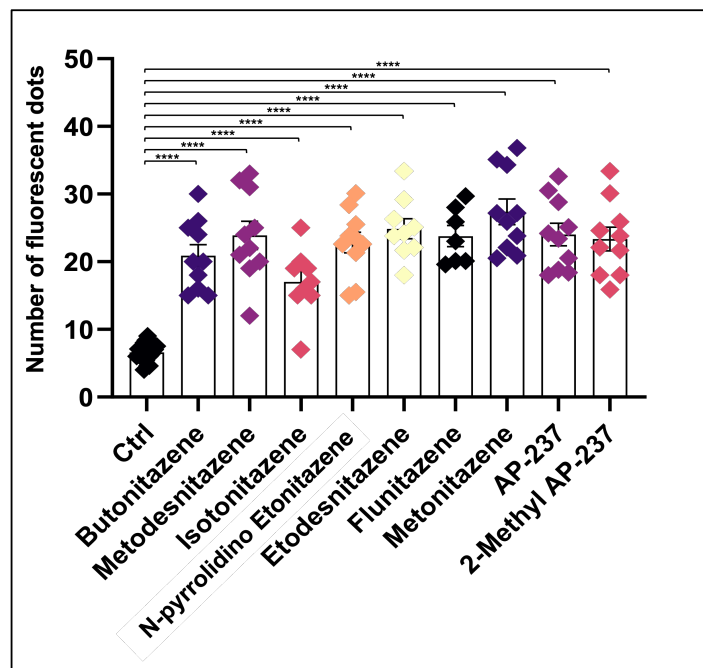


Figure 21: Quantitative analysis of the fluorescent dots indicating the apoptotic/necrotic cells. $N=2$ experiments, $n=10$ samples; **** $p < 0,0001$.

5.4.4.2 Morphological assay

The morphological assay was performed by exposing larvae for 24 hours to 1 μM of each synthetic opioid. No significant difference in mortality between treatment groups and the control groups was observed for all the tested compounds except for larvae exposed to metodesnitazene and N-pyrrolidino etonitazene, in which the survival rate was 87%.

Pericardial edema, yolk sac edema, somite and body axis deformities were observed in all treated larvae, while no malformations were recorded in the control group. These types of morphological defects were already reported for other synthetic opioids^{66,127}.

5.4.4.3 Metabolic assay

In this work, metabolite analysis of the selected synthetic opioid was performed using LC-HRMS with full-scan mode acquisition. Several metabolites were identified, the main metabolic pathways being monohydroxylation, N-dealkylation, and O-dealkylation.

Table 4 summarizes the main metabolites identified for each one of the studied compounds, along with their chemical structure, retention times and calculated exact mass of precursors and product ions. The proposed chemical structure of each metabolite was postulated on the bases of the limited data in literature, m/z , retention time ratio and fragmentation patterns.

<i>Compound Name</i>	<i>Chemical formula</i>	<i>Theoretical mass (m/z)</i>	<i>Experimental mass (m/z)</i>	<i>RT (min)</i>	<i>Major fragments (m/z)</i>
AP-237	$\text{C}_{17}\text{H}_{24}\text{N}_2\text{O}$	273.1961	273.1965	6.8	117.0666 155.1158 91.0515
OH-AP-237	$\text{C}_{17}\text{H}_{24}\text{N}_2\text{O}_2$	289.1911	289.1811	5.9	133.0606 157.1291 87.0895
2-methyl-AP-237	$\text{C}_{18}\text{H}_{26}\text{N}_2\text{O}$	287.2118	287.2120	7.0	117.0663 169.1329 91.0498

OH-2-methyl-AP-237	$C_{18}H_{26}N_2O_2$	303.2067	303.2057	6.0	171.1450 133.0613 101.1026
Isotonitazene	$C_{23}H_{30}N_4O_3$	411.2391	411.2405	7.7	100.1091 72.0785
N-desethyl isotonitazene	$C_{21}H_{26}N_4O_3$	383.2078	383.2068	7.5	72.0779 312.1243
O-dealkyl isotonitazene (4-hydroxynitazene)	$C_{20}H_{24}N_4O_3$	369.1921	369.1929	6.4	100.1115 133.0810 72.0877
Metonitazene	$C_{21}H_{26}N_4O_3$	383.2078	383.2097	7.1	100.1093 72.0784 121.0633
N-desethyl metonitazene	$C_{19}H_{22}N_4O_3$	355.1765	355.1750	6.9	72.0785 121.0617
O-demethyl metonitazene (4-hydroxynitazene)	$C_{20}H_{24}N_4O_3$	369.1921	369.1930	6.4	100.1094 72.0780
Etodesnitazene	$C_{22}H_{29}N_3O$	352.2383	352.2374	6.3	100.1092 72.0765
N-desethyl etodesnitazene	$C_{20}H_{25}N_3O$	324.2070	324.2055	5.9	253.1330 72.0789
Butonitazene	$C_{24}H_{32}N_4O_3$	425.2547	425.2552	9.3	100.1114 72.0802 107.0485
Hydroxy butonitazene	$C_{24}H_{32}N_4O_4$	441.2496	441.2495	7.2	100.1114 72.0803 107.0485
Hydroxy butonitazene	$C_{24}H_{32}N_4O_4$	441.2496	441.2495	9.3	100.1116 72.0804 107.0488
O-desbutyl butonitazene (4-hydroxynitazene)	$C_{20}H_{24}N_4O_3$	369.1921	369.1926	6.4	100.1115 107.0486 72.0803
O-desbutyl N-desethyl butonitazene	$C_{18}H_{20}N_4O_3$	341.1608	341.1613	6.1	72.0803 107.0485 270.0870
N-desethyl butonitazene	$C_{22}H_{28}N_4O_3$	397.2234	397.2238	9.0	72.0806 326.1499 107.0489

Metodesnitazene	C ₂₁ H ₂₇ N ₃ O	338.2227	338.2214	5.4	100.1114 72.0803 121.0643
O-demethyl metodesnitazene	C ₂₀ H ₂₅ N ₃ O	324.2070	324.2066	4.1	100.1116 72.0804 86.0960
N-desethyl metodesnitazene	C ₁₉ H ₂₃ N ₃ O	310.1921	310.1921	4.9	239.1181 72.0805 131.0601 121.0644
Flunitazene	C ₂₀ H ₂₃ FN ₄ O ₂	371.1878	371.1886	7.6	100.1116 109.0444 72.0805
N-desethyl flunitazene	C ₁₈ H ₁₉ FN ₄ O ₂	343.1565	343.1561	7.3	72.0806 109.0444
N-pyrrolidino etonitazene	C ₂₂ H ₂₆ N ₄ O ₃	395.2078	395.2081	7.9	98.0961 107.0488 135.0801
N-pyrrolidino etonitazene dehydrogenation	C ₂₂ H ₂₄ N ₄ O ₃	393.1921	393.1925	7.7	96.0804 107.0488 135.0800
O-desethyl N-pyrrolidino etonitazene	C ₂₀ H ₂₂ N ₄ O ₃	367.1765	367.1750	6.2	98.0959 107.0485

Table 4: List of tentative identified compounds.

Furthermore, exemplary chromatograms and full scan High resolution accurate mass (HRAM) mass spectra of precursors ions, as well as identified metabolites of butonitazene and metodesnitazene are depicted in figure 22-26 since no data are present in literature regarding their metabolic fate (as for flunitazene and N-pyrrolidino etonitazene).

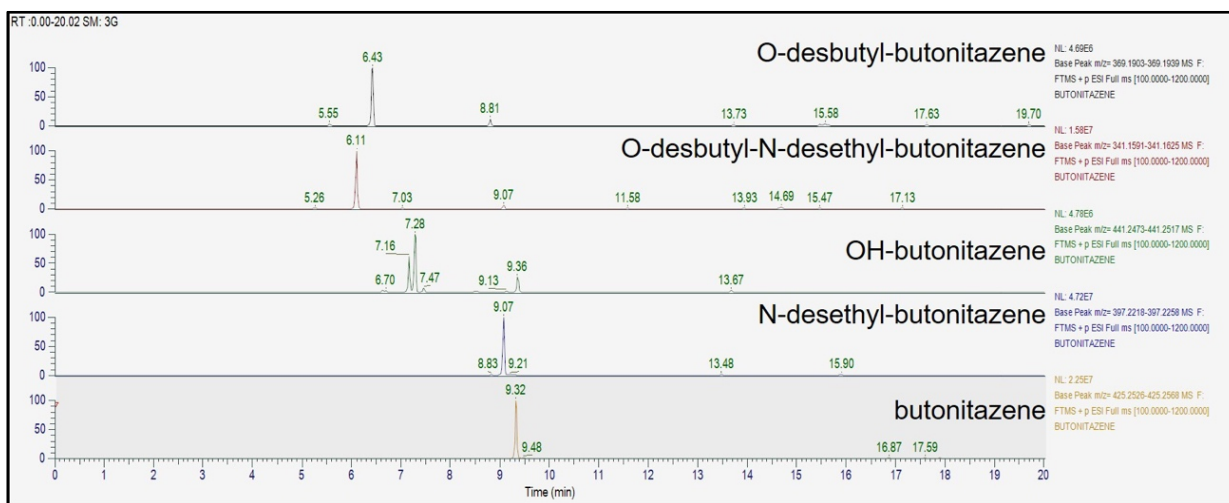


Figure 22: LC-MS/MS analysis of extract of zebrafish larvae incubated for 24 hours with 1 μ M butonitazene.

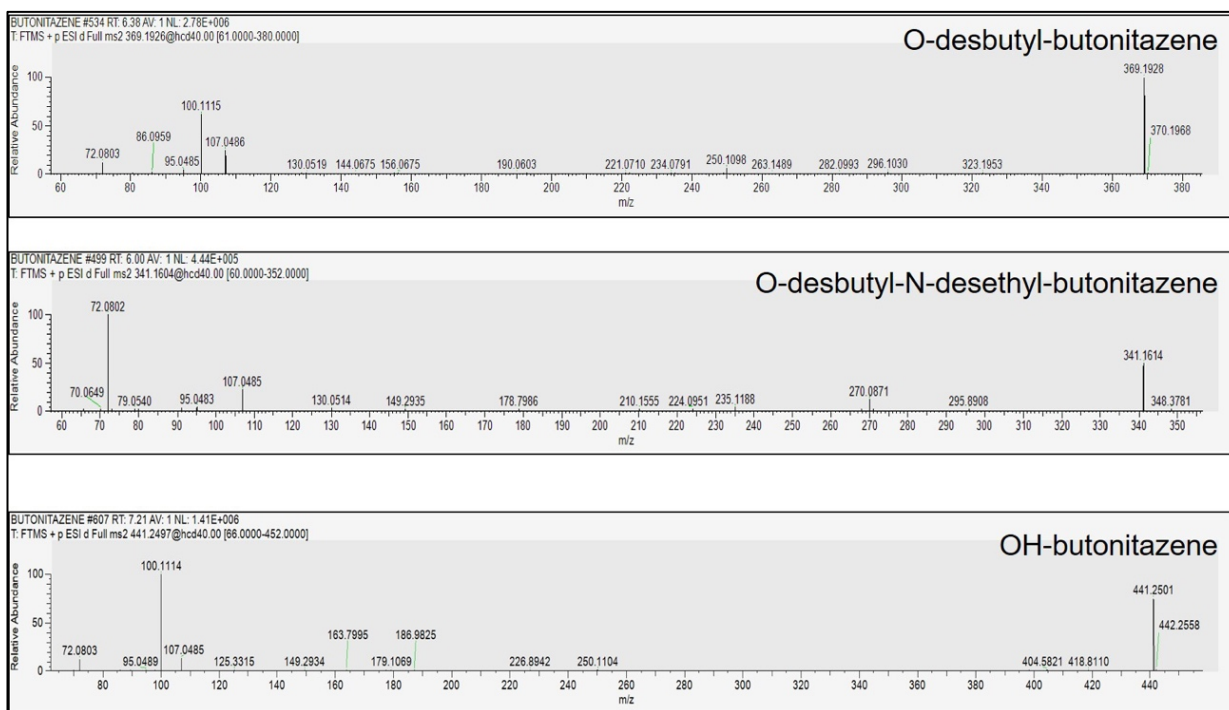


Figure 23: Full scan HRAM MS2 mass spectrum for butonitazene metabolites.

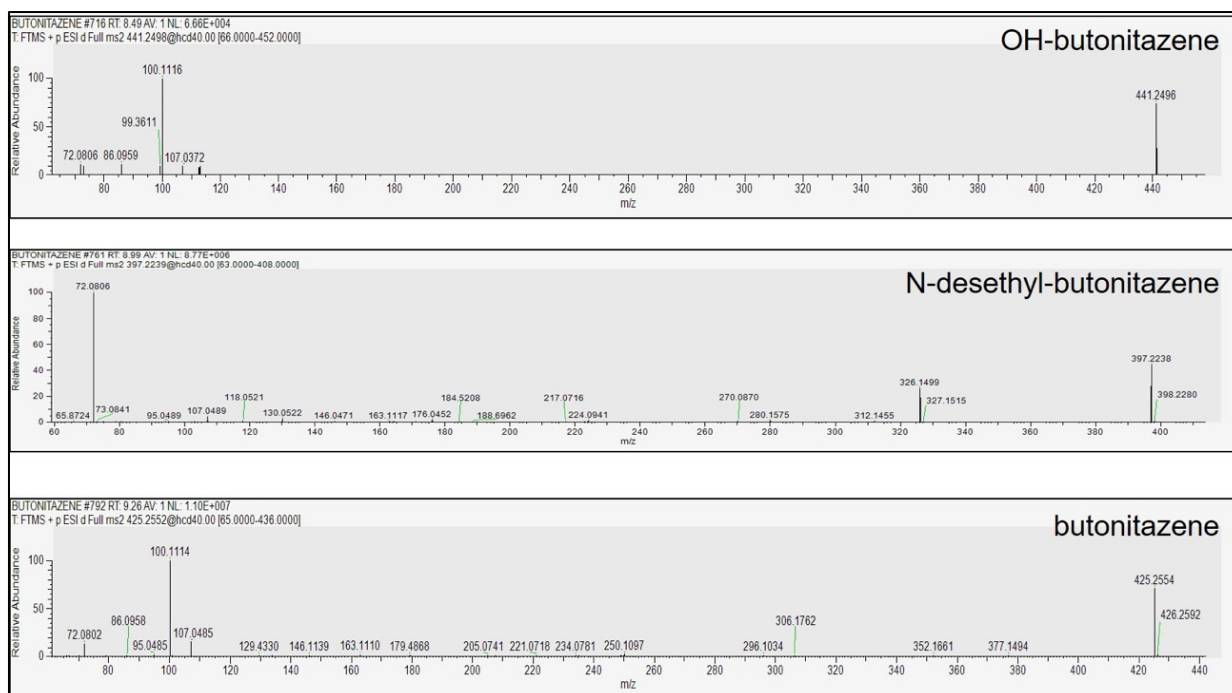


Figure 24: Full scan HRAM MS2 mass spectrum for butonitazene metabolites.

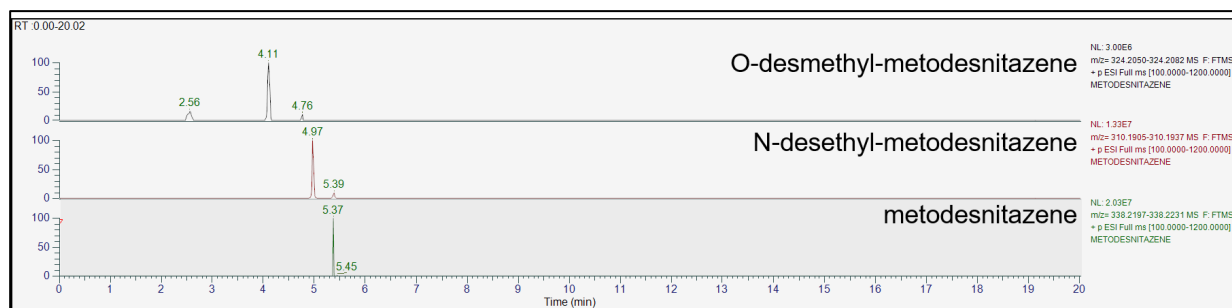


Figure 25: LC-MS/MS analysis of extract of zebrafish larvae incubated for 24 hours with 1 μ M metodesnitazene.

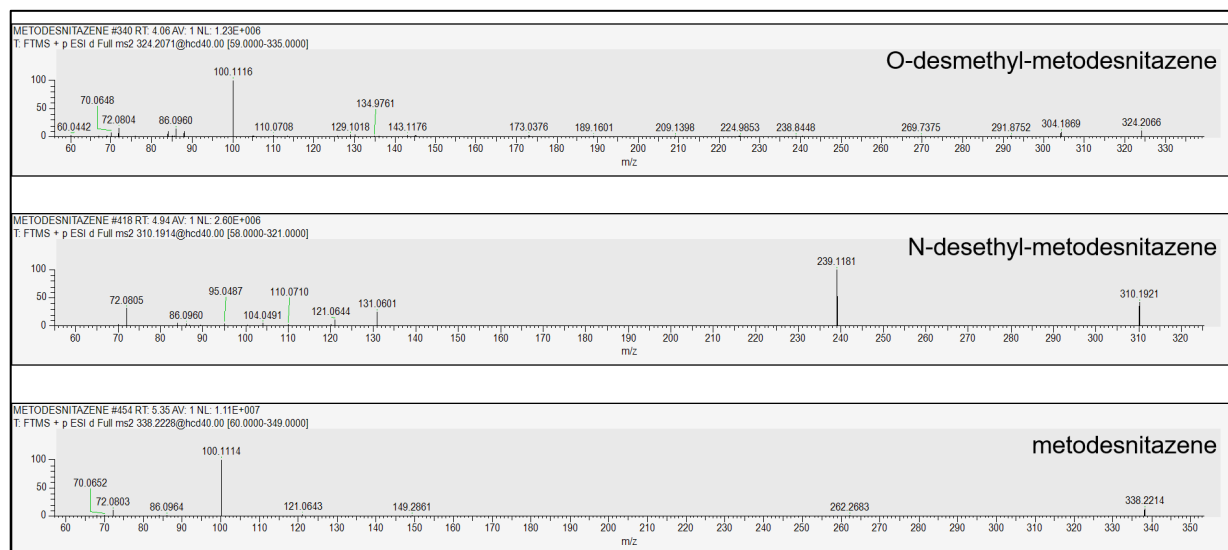


Figure 26: Full scan HRAM MS2 mass spectrum for metodesnitazene metabolites.

As regard AP-237 and 2-methyl-AP-237, the two compounds were metabolized by zebrafish larvae in their monohydroxylated form. The hydroxylation occurred on the cinnamyl chain and was confirmed by the presence of fragment 133.0606 m/z, representing the hydroxylated cinnamyl chain fragment for both AP-237 and 2-methyl-AP-237.

The metabolic pathway of benzimidazole opioids is depicted in figure 27.

For isotonitazene, ZL produced only two metabolites through dealkylation either in N- or in O- position. In N-desethyl isotonitazene, the predominant fragments are 72.0779 m/z and 312.1243 m/z, representing the diethylamine and the counterpart of the molecule. On the contrary, in O-dealkyl isotonitazene, the most abundant fragment is 100.115 m/z, corresponding to triethylamine.

As its analog (isotonitazene), metonitazene underwent N-dealkylation and O-demethylation, forming 4-hydroxy metonitazene. In N-dealkylation, the fragment 72.0785 m/z represents the diethylamine portions and the fragment 121.0617 m/z corresponds to the methoxybenzyl moiety.

N-desethylation was detectable also in etodesnitazene, where fragmentation showed clearly the fragment 253.1330 m/z, representing the loss of the diethylamine chain (72.0789 m/z) from the benzimidazole core.

Larvae treated with butonitazene showed four metabolites produced by dealkylation, in N- and/or O- position and monohydroxylation, which can occur in two different positions, as reflected by the two distinctive retention time. A significant fragment present in both the N-dealkyl and in N-dealkyl O-dealkyl metabolites was 107.0485 m/z, which is the hydroxybenzyl moiety.

Concerning metodesnitazene, in larvae extracts were observed both two dealkyl derivatives, namely O- demethyl metodesnitazene and N-desethyl metodesnitazene. The latter was confirmed by the presence of 72.0805 m/z and 121.0644 m/z, representing the methoxybenzyl group, as major fragments.

The N-desethyl metabolite (343.1561 m/z) was the only one metabolite identified in ZL treated with flunitazene: also, for this compound 72.0806 m/z and 109.0444 m/z (fluorobenzyl) represent the main fragments.

Lastly, N-pyrrolidino etonitazene was metabolized through a dehydrogenation with the introduction of a double bond in the 2-pyrrolidin-1-ethyl structure, as confirmed

by the presence of the fragment 96.0804 m/z. Another identified metabolite was the result of the O-dealkylation with the loss of the ethyl chain (fragment 107.0485 m/z).

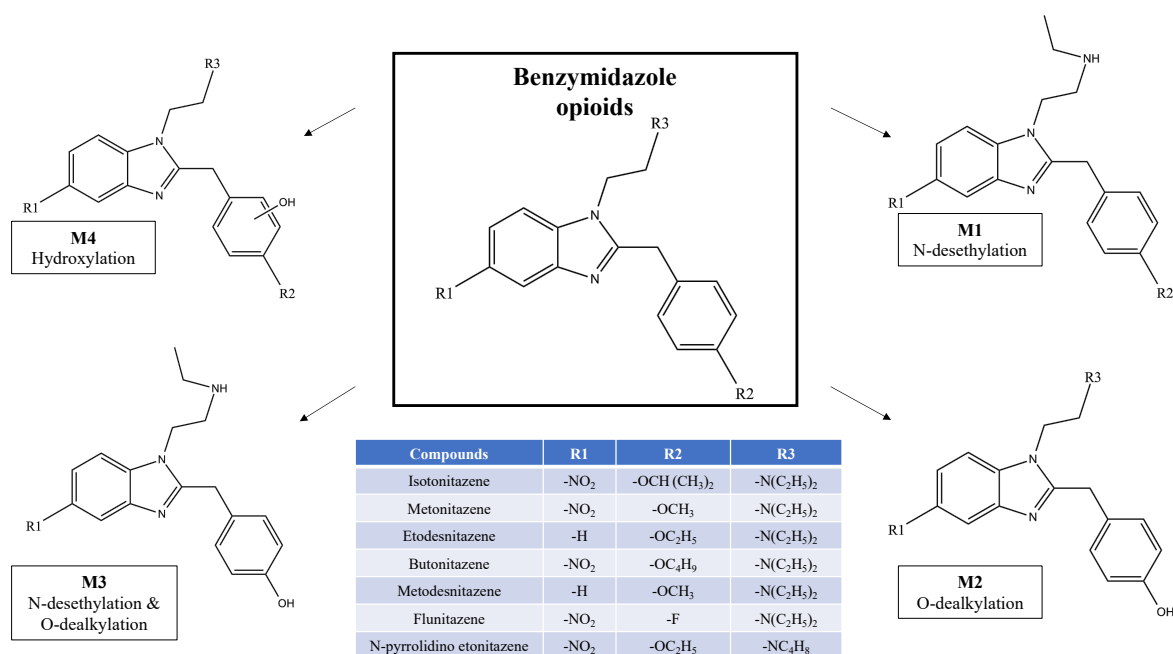


Figure 27: Metabolic pathway of benzimidazole opioids

5.4.5 Discussion

In the present study, zebrafish embryos were treated with a number of opioids, and the effects of these treatments on cell death were assessed by using acridine orange-fluorescent staining.

Interestingly, the localization of fluorescence signals in the body of the larvae, allowed to identify regions characterized by high levels of cellular death. Moreover, the quantification of the fluorescent spots can provide a rapid screening system for compounds that can induce cellular death by apoptosis or necrosis. With the acridine orange assay, we found that the exposure of zebrafish embryos to opioids results in an overall increase in cell death during development, as indicated by the presence of various scattered spots. It is worth noting that all the opioids used for the acridine orange test were administrated at very low concentration (0.1 μ M) to avoid the presence of embryonal malformations and lethality. This approach allowed us to conclude that all the analysed compounds have an intrinsic pro-

apoptotic/necrotic effect not associable with the presence of phenotypic alterations that can potentially interfere with this analysis.

For the morphological evaluation, the concentration of 1 μM was chosen on the bases of previous study on fentanyl and other fentanyl analogs. The assay showed that the survival rate of zebrafish embryos treated with the different synthetic opioids was higher than 87%, indicating that the synthetic opioids have low toxicity towards common cells.

Regarding the metabolic analysis, the most observed biotransformation and the relative metabolites identified are in line with the limited data present in the literature. As per AP-237, our results are in accordance with a study on rats and rabbits, where the main metabolic pathway was represented by the *p*-hydroxylation on the benzene ring in the cinnamyl moiety^{113,128}. Concerning its methyl derivative, Hassanien *et al.* found that the only metabolic route for the compound in human liver microsomes is the hydroxylation, which could occur on various positions, i.e. on the cinnamyl chain, piperazine ring or acyl chain¹²⁹.

As concern isotonitazene, in 2020 Krotulski and colleagues observed that N-dealkylation and O-dealkylation or the combination of them were the biotransformation detectable in human urine samples. According to authors suggestions and our findings, N-desethyl isotonitazene may be an appropriate metabolite marker to monitor isotonitazene consumption^{119,130}.

Metonitazene metabolism was studied in several forensic post-mortem cases by Krotulski *et al.*, analyzing urine, blood and vitreous humor¹³¹. The comparison with our results showed some common points. Indeed, the presence of N-desethyl metonitazene was prominent in urine and vitreous humor samples. Furthermore, 4-hydroxy metonitazene (O-demethyl metonitazene) was a common metabolite in all the cases examined, however less abundant than the former. Conversely, the nitro-reduction, which is another possible biotransformation in blood samples, was not observed.

Despite the presence of an alkoxy substituent, O-dealkylation was not detectable in larvae exposed to etodesnitazene, whereas only N-desethyl etodesnitazene was found. The metabolism of this drug was studied by Grigoryev *et al.* in rat serum and urine¹²¹. Although a higher quantity of possible biotransformation highlighted,

authors concluded that the most likely forming metabolites in human could be mono-desethylated and/or monohydroxylated metabolites¹³².

Among the nine drugs studied, butonitazene showed the highest number of metabolites. Moreover, it was noticeable that it was the only substance, within the benzimidazole class, which formed two monohydroxylated metabolites. A possible explanation of the presence of hydroxy butonitazene might be due to the great lipophilia of the molecule (logP estimated to 5.2¹³³), hence favoring the excretion by adding the hydroxyl group (-OH).

To the best of authors' knowledge, no information regarding the metabolism of butonitazene, metodesnitazene, flunitazene, and N-pyrrolidino etonitazene has so far been reported. Previous studies have been focused on chemical and pharmacological characterization^{120,122,123} and/or intoxication or fatal cases^{119,131,134}.

6. FINAL CONCLUSION

In the present PhD thesis project, a new approach for evaluating toxicity of new synthetic opioids based on zebrafish larvae was tested. The present study had been structured in three main phases.

The first part of the project was dedicated to the development of the experimental protocol and fentanyl was chosen as reference compound of the class of opioids, because its pharmacological properties were already clarified in both humans and in animal models. Zebrafish larvae were exposed to different concentrations of fentanyl to set-up the experimental protocol for the evaluation of morphological toxicity, metabolic pathway and behavioral effects. In parallel, mice were treated with the same compound for a comparison of ZL results with those obtained with a well-established animal model.

Behavioral tests and metabolite production in ZL were consistent with the results in mice. Using ZL it was possible also to highlight the presence of several morphological abnormalities when exposed to high fentanyl doses (50, 100 μ M).

Starting from these promising results, a new study was then conducted with two fentanyl analogs (2-furanylfentanyl and ocfentanil), selected among the new synthetic opioids whose behavioral effects, toxicity and metabolism data were scarce. Again, to confirm the validity of the model, ZL results had been compared to those obtained in mice. In particular, the behavioral assay showed a decrease in basal locomotor activity in zebrafish, whereas in mice this effect was evident only after a mechanical stimulus.

The last part of the thesis was focused on the evaluation of the metabolism of ZL on a panel of 9 different new synthetic opioids. The study showed that the tested drugs are metabolized in zebrafish embryos by pathways similar to those expected in humans.

Overall, the results of this thesis project strongly support the hypothesis that ZL can be used as an experimental model for assessing the effects of new synthetic opioids. Indeed, ZL can provide, at least in a preliminary phase, useful information on different pharmaco-toxicological aspects of NSO.

Moreover, ZL can be regarded as a suitable animal model for large-scale screening of new psychoactive drugs to be performed before the completion of more formal

studies in mammals. In particular, ZL could be exploited for the identification of metabolites of new drugs to be used as biomarkers of recent use in humans.

Results of this thesis have been subjects of scientific publications and oral communication at national and international congress as summarized below.

Scientific publications:

- Pesavento S, Bilel S, Murari M, Gottardo R, Arfè R, Tirri M, Panato A, Tagliaro F, Marti M. Zebrafish larvae: A new model to study behavioural effects and metabolism of fentanyl, in comparison to a traditional mice model. *Med Sci Law*. 2022 Jul;62(3):188-198. doi: 10.1177/00258024221074568. Epub 2022 Jan 18. PMID: 35040690.
Contribution statement – Murari M: investigation and data interpretation.
- Bilel S, Murari M, Pesavento S, Arfè R, Tirri M, Torroni L, Marti M, Tagliaro F, Gottardo R. Toxicity and behavioural effects of ocfentanil and 2-furanylfentanyl in zebrafish larvae and mice. *Neurotoxicology*. 2023 Mar;95:83-93. doi: 10.1016/j.neuro.2023.01.003. Epub 2023 Jan 10. PMID: 36634872.
Contribution statement – Murari M: data acquisition, investigation and original draft preparation.
- Murari M, Pesavento S, Greco F, Vettori A, Tagliaro F, Gottardo R. Study of metabolism and potential toxicity of nine synthetic opioid analogs using the zebrafish larvae model. *Drug Test Anal*. 2023 Nov 2. doi: 10.1002/dta.3590. Epub ahead of print. PMID: 37916273.

Oral communications:

- “Studio in vivo del metabolismo e degli effetti comportamentali del fentanyl mediante il nuovo modello animale dello Zebrafish” oral presentation at the congress of *Gruppo dei Tossicologi Forensi Italiani (GTFI)* held in Vicenza (IT), 28-29/10/2021.
- “Zebrafish larvae as a model to study the metabolism of New Psychoactive Substances: a comparison with mice by using High Resolution Mass Spectrometry” oral presentation at the *3rd Autumn Meeting for Young Chemists in Biomedical Sciences (AMYC-BIOMED)* held in Napoli (IT), 17-19/10/2022.
- “The use of zebrafish early life stage to investigate the metabolism and toxic effect of nine NPS with opioid effects” oral presentation at the 60°

International meeting of the International Association of Forensic Toxicologists (TIAFT) held in Rome (IT), 27-31/08/2023.

REFERENCES

1. United Nations Office on Drugs and Crime (UNODC). United Nations Office on Drugs and Crime. Global smart update 2016. *2016*.
2. Peacock, A. *et al.* New psychoactive substances: challenges for drug surveillance, control, and public health responses. *The Lancet* **394**, 1668–1684 (2019).
3. Shafi, A., Berry, A. J., Sumnall, H., Wood, D. M. & Tracy, D. K. New psychoactive substances: a review and updates. *Ther Adv Psychopharmacol* **10**, 1–21 (2020).
4. United Nations Office on Drugs and Crime (UNODC). *World Drug Report 2019*. (2019).
5. European Monitoring Centre for Drugs and Drug Addiction. *European Drug Report 2019: trends and developments*. (2019).
6. United Nations Office on Drugs and Crime (UNODC). UNODC Early Warning Advisory on NPS - Summary Dashboard. <https://www.unodc.org/LSS/Page/NPS/DataVisualisations> (2023).
7. United Nations Office on Drugs and Crime (UNODC). *The Challenge of New Psychoactive Substances; Global SMART Programme*. http://www.unodc.org/documents/scientific/NPS_Report.pdf (2013).
8. United Nations Office on Drugs and Crime (UNODC). *Global Synthetic Drugs Assessment*. (2017).
9. Lovrecic, B. *et al.* Non-medical use of novel synthetic opioids: A new challenge to public health. *Int J Environ Res Public Health* **16**, 1–21 (2019).
10. Gardner, E. A., McGrath, S. A., Dowling, D. & Bai, D. The Opioid Crisis: Prevalence and Markets of Opioids. *Forensic Sci Rev* **34**, 43–70 (2022).
11. Weedn, V. W., Elizabeth Zaney, M., McCord, B., Lurie, I. & Baker, A. Fentanyl-related substance scheduling as an effective drug control strategy. *J Forensic Sci* **66**, 1186–1200 (2021).
12. Prekupec, M. P., Mansky, P. A. & Baumann, M. H. Misuse of Novel Synthetic Opioids: A Deadly New Trend. *Journal of Addiction Medicine* Preprint at <https://doi.org/10.1097/ADM.0000000000000324> (2017).
13. Zhuang, Y. *et al.* Molecular recognition of morphine and fentanyl by the human μ -opioid receptor. *Cell* **185**, 4361-4375.e19 (2022).
14. Trescot, A. M., Datta, S., Lee, M. & Hansen, H. Opioid pharmacology. *Pain Physician* **11**, S133-53 (2008).
15. Albores-García, D. & Cruz, S. L. Fentanyl and other New Psychoactive Synthetic Opioids. Challenges to Prevention and Treatment. *Rev Invest Clin* **75**, 93–104 (2023).
16. Kuczyńska, K., Grzonkowski, P., Kacprzak, Ł. & Zawilska, J. B. Abuse of fentanyl: An emerging problem to face. *Forensic Science International* 207–214 Preprint at <https://doi.org/10.1016/j.forsciint.2018.05.042> (2018).

17. Richter, L. H. J., Maurer, H. H. & Meyer, M. R. New psychoactive substances: Studies on the metabolism of XLR-11, AB-PINACA, FUB-PB-22, 4-methoxy- α -PVP, 25-I-NBOMe, and meclonazepam using human liver preparations in comparison to primary human hepatocytes, and human urine. *Toxicol Lett* **280**, 142–150 (2017).
18. Meyer, M. R. New psychoactive substances: an overview on recent publications on their toxicodynamics and toxicokinetics. *Arch Toxicol* **90**, 2421–2444 (2016).
19. Morbiato, E. *et al.* Potential of the zebrafish model for the forensic toxicology screening of NPS: A comparative study of the effects of APINAC and methiopropamine on the behavior of zebrafish larvae and mice. *Neurotoxicology* **78**, 36–46 (2020).
20. Hill, A. J., Teraoka, H., Heideman, W. & Peterson, R. E. Zebrafish as a model vertebrate for investigating chemical toxicity. *Toxicological Sciences* 6–19 Preprint at <https://doi.org/10.1093/toxsci/kfi110> (2005).
21. McClure, M. Development and evolution of melanophore patterns in fishes of the Genus *Danio* (Teleostei: Cyprinidae). *J Morphol* **241**, 83–105 (1999).
22. Watanabe, M. *et al.* Spot pattern of leopard *Danio* is caused by mutation in the zebrafish connexin41.8 gene. *EMBO Rep* **7**, 893–897 (2006).
23. Spence, R., Gerlach, G., Lawrence, C. & Smith, C. The behaviour and ecology of the zebrafish, *Danio rerio*. *Biological Reviews* **83**, 13–34 (2008).
24. Kimmel, C. B., Ballard, W. W., Kimmel, S. R., Ullmann, B. & Schilling, T. F. Stages of embryonic development of the zebrafish. *Developmental Dynamics* **203**, 253–310 (1995).
25. de Souza Anselmo, C., Sardela, V. F., de Sousa, V. P. & Pereira, H. M. G. Zebrafish (*Danio rerio*): A valuable tool for predicting the metabolism of xenobiotics in humans? *Comparative Biochemistry and Physiology Part - C: Toxicology and Pharmacology* (212) 34-46 Preprint at <https://doi.org/10.1016/j.cbpc.2018.06.005> (2018).
26. Sipes, N. S., Padilla, S. & Knudsen, T. B. Zebrafish-As an integrative model for twenty-first century toxicity testing. *Birth Defects Res C Embryo Today* **93**, 256–267 (2011).
27. Murray, S. A. *et al.* Mouse gestation length is genetically determined. *PLoS One* **5**, (2010).
28. Kalueff, A. V., Stewart, A. M. & Gerlai, R. Zebrafish as an emerging model for studying complex brain disorders. *Trends Pharmacol Sci* **35**, 63–75 (2014).
29. Diekmann, H. & Hill, A. ADMETox in zebrafish. *Drug Discov Today Dis Models* **10**, e31–e35 (2013).
30. Goldstone, J. V. *et al.* Identification and developmental expression of the full complement of Cytochrome P450 genes in Zebrafish. *BMC Genomics* (2010) doi:10.1186/1471-2164-11-643.
31. Hill, A. Zebrafish in Drug Discovery: Safety Assessment. in *Drug Discovery and Evaluation: Safety and Pharmacokinetic Assays* 605–629 (Springer Berlin Heidelberg, 2013). doi:10.1007/978-3-642-25240-2_22.

32. Huang, H. & Wu, Q. Cloning and comparative analyses of the zebrafish Ugt repertoire reveal its evolutionary diversity. *PLoS One* **5**, (2010).
33. Liu, T.-A. *et al.* Zebrafish as a Model for the Study of the Phase II Cytosolic Sulfotransferases. *Curr Drug Metab* **11**, 538–546 (2010).
34. Postlethwait, J. H. *et al.* Zebrafish Comparative Genomics and the Origins of Vertebrate Chromosomes. *Genome Res* **10**, 1890–1902 (2000).
35. Walsh, R. N. & Cummins, R. A. The Open-Field Test: a critical review. *Psychol Bull* **83**, 482–504 (1976).
36. Ahmad, F. & Richardson, M. K. Exploratory behaviour in the open field test adapted for larval zebrafish: Impact of environmental complexity. *Behavioural Processes* **92**, 88–98 (2013).
37. Rosemberg, D. B. *et al.* Differences in spatio-temporal behavior of zebrafish in the open tank paradigm after a short-period confinement into dark and bright environments. *PLoS One* **6**, (2011).
38. Blaser, R. E., Chadwick, L. & McGinnis, G. C. Behavioral measures of anxiety in zebrafish (*Danio rerio*). *Behavioural Brain Research* **208**, 56–62 (2010).
39. Basnet, R. M., Zizioli, D., Taweedet, S., Finazzi, D. & Memo, M. Zebrafish larvae as a behavioral model in neuropharmacology. *Biomedicines* **7**, (2019).
40. Ganzen, L., Venkatraman, P., Pang, C. P., Leung, Y. F. & Zhang, M. Utilizing zebrafish visual behaviors in drug screening for retinal degeneration. *Int J Mol Sci* **18**, 1–21 (2017).
41. Dong, M. W. 3 HPLC instrumentation in pharmaceutical analysis: Status, advances, and trends. in 47–75 (2005). doi:10.1016/S0149-6395(05)80047-9.
42. Pragst, F. Chapter 13. in *High performance liquid chromatography in forensic toxicological analysis, Second Edition, vol 6* (2006).
43. Skoog, D., Holler, J. & Crouch, S. Principles of Instrumental Analysis. in (2007).
44. Griffiths, J. A Brief History of Mass Spectrometry. *Anal Chem* **80**, 5678–5683 (2008).
45. Gross, J. *Mass Spectrometry A Textbook Third Edition. Analytical Chemistry* vol. 56 (2017).
46. Bruker Daltonics. Introduction to Ion Trap Mass Spectrometry Toxyper Key Components. 1–30 (2017).
47. Wallace Geer, M. A. & McCord, J. P. High-resolution mass spectrometry. in *Breathborne Biomarkers and the Human Volatilome* Chapter 16 (2016).
48. Nari, H. & Clarke, W. *Mass Spectrometry for the Clinical Laboratory*. (2017).
49. Kicman, A. T., Parkin, M. C. & Iles, R. K. An introduction to mass spectrometry based proteomics-Detection and characterization of gonadotropins and related molecules. *Mol Cell Endocrinol* **260–262**, 212–227 (2007).
50. de Hoffmann, E., Charette, J. & Stroobant, V. *Mass Spectrometry: Principles and Applications*. (1996).

51. Kingdon, K. H. A method for the neutralization of electron space charge by positive ionization at very low gas pressures. *Physical Review* **21**, 408–418 (1923).
52. Makarov, A. Electrostatic axially harmonic orbital trapping: A high-performance technique of mass analysis. *Anal Chem* **72**, 1156–1162 (2000).
53. Scigelova, M. & Makarov, A. Orbitrap mass analyzer - Overview and applications in proteomics. *Proteomics* **1**, 16–21 (2006).
54. Gross, J. *Spettrometria di Massa*. (2016).
55. Thermo Scientific. Orbitrap Fusion Lumos Tribrid Mass Spectrometer. *Product Specifications* 1–13 (2015).
56. Medhe, S. Mass Spectrometry: Detectors Review. *Chemical and Biomolecular Engineering* **3**, 51–58 (2018).
57. National Center for Biotechnology Information. PubChem Compound Summary for CID 3345, Fentanyl. <https://pubchem.ncbi.nlm.nih.gov/compound/Fentanyl>. (2023).
58. Stanley, T. H. The fentanyl story. *Journal of Pain* **15**, 1215–16 (2014).
59. Comer, S. D. & Cahill, C. M. Fentanyl: Receptor pharmacology, abuse potential, and implications for treatment. *Neuroscience and Biobehavioral Reviews* Preprint at <https://doi.org/10.1016/j.neubiorev.2018.12.005> (2019).
60. Noyes, P. D., Haggard, D. E., Gonnerman, G. D. & Tanguay, R. L. Advanced morphological - behavioral test platform reveals neurodevelopmental defects in embryonic zebrafish exposed to comprehensive suite of halogenated and organophosphate flame retardants. *Toxicological Sciences* **145**, 177–95 (2015).
61. Bilel, S. *et al.* The novel fentanyl-analog “Acrylofentanyl” impairs motor, sensorimotor and cardiovascular functions in mice. *Pharmadvances* **2**, (2020).
62. Ossato, A. *et al.* Neurological, sensorimotor and cardiorespiratory alterations induced by methoxetamine, ketamine and phencyclidine in mice. *Neuropharmacology* **141**, 167–180 (2018).
63. Bilel, S. *et al.* In vitro and in vivo pharmacological characterization of the synthetic opioid MT-45. *Neuropharmacology* **171**, 108110 (2020).
64. Gampfer, T. M. *et al.* Toxicokinetics and toxicodynamics of the fentanyl homologs cyclopropanoyl-1-benzyl-4'-fluoro-4-anilinopiperidine and furanoyl-1-benzyl-4-anilinopiperidine. *Arch Toxicol* **94**, 2009–2025 (2020).
65. Curtis, M. J. *et al.* Experimental design and analysis and their reporting II: updated and simplified guidance for authors and peer reviewers. *Br J Pharmacol* **175**, 987–993 (2018).
66. Kirla, K. T. *et al.* Zebrafish early life stages as alternative model to study ‘designer drugs’: Concordance with mammals in response to opioids. *Toxicol Appl Pharmacol* **419**, 115483 (2021).
67. Cooman, T., Bergeron, S. A., Coltogirone, R., Horstick, E. & Arroyo, L. Evaluation of fentanyl toxicity and metabolism using a zebrafish model. *Journal of Applied Toxicology* (2021) doi:10.1002/jat.4253.

68. Akhtar, M. T. *et al.* Developmental effects of cannabinoids on zebrafish larvae. *Zebrafish* **10**, 283–293 (2013).
69. Antkiewicz, D. S., Burns, C. G., Carney, S. A., Peterson, R. E. & Heideman, W. Heart malformation is an early response to TCDD in embryonic zebrafish. *Toxicological Sciences* **84**, 368–377 (2005).
70. Achenbach, J. C. *et al.* Analysis of the Uptake, Metabolism, and Behavioral Effects of Cannabinoids on Zebrafish Larvae. *Zebrafish* **15**, 349–360 (2018).
71. MacPhail, R. C. *et al.* Locomotion in larval zebrafish: Influence of time of day, lighting and ethanol. *Neurotoxicology* **289**, 207–214 (2009).
72. Kalueff, A. V. *The rights and wrongs of zebrafish: Behavioral phenotyping of zebrafish. The Rights and Wrongs of Zebrafish: Behavioral Phenotyping of Zebrafish* (2017). doi:10.1007/978-3-319-33774-6.
73. Zaig, S., Scarpellini, C. & Montandon, G. Respiratory depression and analgesia by opioid drugs in freely-behaving larval zebrafish. *Elife* **10**, 1–20 (2021).
74. Evans, J. R., Torres-Pérez, J. V., Miletto Petrazzini, M. E., Riley, R. & Brennan, C. H. Stress reactivity elicits a tissue-specific reduction in telomere length in aging zebrafish (*Danio rerio*). *Sci Rep* **11**, 1–11 (2021).
75. Stewart, A. M. & Kalueff, A. V. The behavioral effects of acute Δ^9 -tetrahydrocannabinol and heroin (diacetylmorphine) exposure in adult zebrafish. *Brain Res* **1543**, 109–119 (2014).
76. Stewart, A. *et al.* Pharmacological modulation of anxiety-like phenotypes in adult zebrafish behavioral models. *Prog Neuropsychopharmacol Biol Psychiatry* **35**, 1421–1431 (2011).
77. Bao, W. *et al.* Opioid Neurobiology, Neurogenetics and Neuropharmacology in Zebrafish. *Neuroscience* **404**, 218–232 (2019).
78. Di Chiara, G. & Imperato, A. Opposite effects of mu and kappa opiate agonists on dopamine release in the nucleus accumbens and in the dorsal caudate of freely moving rats. *Journal of Pharmacology and Experimental Therapeutics* **244**, 1067–1080 (1988).
79. Rodríguez-Arias, M., Broseta, I., Aguilar, M. A. & Miñarro, J. Lack of specific effects of selective D1 and D2 dopamine antagonists vs. risperidone on morphine-induced hyperactivity. *Pharmacol Biochem Behav* **66**, 189–197 (2000).
80. Matsui, A., Jarvie, B. C., Robinson, B. G., Hentges, S. T. & Williams, J. T. Separate GABA afferents to dopamine neurons mediate acute action of opioids, development of tolerance, and expression of withdrawal. *Neuron* **82**, 1346–1356 (2014).
81. Martin, D. C., Introna, R. P. & Aronstam, R. S. Fentanyl and sufentanil inhibit agonist binding to 5-HT_{1A} receptors in membranes from the rat brain. *Neuropharmacology* **30**, 323–327 (1991).
82. Gurtu, S. MU receptor-serotonin link in opioid induced hyperactivity in mice. *Life Sci* **46**, 1539–1544 (1990).
83. Yadav, S. K., Kumar, D., Kumar, P., Gupta, P. K. & Bhattacharya, R. Biochemical, Oxidative, and Physiological Changes Caused by Acute Exposure of Fentanyl and Its 3 Analogs in Rodents. *Int J Toxicol* **37**, 28–37 (2018).

84. Lui, P.-W., Lee, T.-Y. & Chan, S. H. H. Involvement of locus coeruleus and noradrenergic neurotransmission in fentanyl-induced muscular rigidity in the rat. *Neurosci Lett* **96**, 114–119 (1989).
85. Kinshella, M. L. W., Gauthier, T. & Lysyshyn, M. Rigidity, dyskinesia and other atypical overdose presentations observed at a supervised injection site, Vancouver, Canada. *Harm Reduct J* **15**, 1–7 (2018).
86. Kanamori, T. *et al.* Use of hepatocytes isolated from a liver-humanized mouse for studies on the metabolism of drugs: application to the metabolism of fentanyl and acetylfentanyl. *Forensic Toxicol* **36**, 467–475 (2018).
87. Wallgren, J. *et al.* Structure Elucidation of Urinary Metabolites of Fentanyl and Five Fentanyl Analogs using LC-QTOF-MS, Hepatocyte Incubations and Synthesized Reference Standards. *J Anal Toxicol* **44**, 993–1003 (2020).
88. Wilde, M. *et al.* Metabolic pathways and potencies of new fentanyl analogs. *Frontiers in Pharmacology* Preprint at <https://doi.org/10.3389/fphar.2019.00238> (2019).
89. Labroo, R., Paine, M., Thummel, K. & Kharasch, E. Fentanyl Metabolism by Human Hepatic and Intestinal Cytochrome P450 3A4: Implications for Interindividual Variability in Disposition, Efficacy, and Drug Interactions. *Drug Metabolism and Disposition* **25**, 1072–1080 (1997).
90. Misailidi, N. *et al.* Fentanyls continue to replace heroin in the drug arena: the cases of ocfentanil and carfentanil. *Forensic Toxicology* Preprint at <https://doi.org/10.1007/s11419-017-0379-4> (2018).
91. Misailidi, N. *et al.* A GC–MS method for the determination of furanylfentanyl and ocfentanil in whole blood with full validation. *Forensic Toxicol* (2019) doi:10.1007/s11419-018-0449-2.
92. Glass, P., Camporesi, E., Martel, D. & Afifi, M. The analgesic efficacy of A3217. *Anesthesiology* **71**, A32 (1989).
93. Fletcher, J. E., Sebel, P. S., Murphy, M. R., Mick, S. A. & Fein, S. Comparison of ocfentanil and fentanyl as supplements to general anesthesia. *Anesth Analg* (1991) doi:10.1213/00000539-199111000-00019.
94. Kanamori, T. *et al.* Detection and confirmation of the ring-opened carboxylic acid metabolite of a new synthetic opioid furanylfentanyl. *Forensic Toxicol* (2021) doi:10.1007/s11419-020-00546-7.
95. Goggin, M. M., Nguyen, A. & Janis, G. C. Identification of unique metabolites of the designer opioid furanyl fentanyl. *J Anal Toxicol* **41**, 367–375 (2017).
96. Huang B.-S., Terrell R. C., Deutsche K. H., Kudzma L. V., L. N. L. N-aryl-n-(4-piperidinyl)amides and pharmaceutical compositions and method employing such compounds. *General Pharmacology: The Vascular System* (1987) doi:10.1016/0306-3623(87)90295-3.
97. Slovenian National Forensic Laboratory. *NPS and related compounds. Analytical reports.* (2016).
98. Varshneya, N. B. *et al.* Respiratory depressant effects of fentanyl analogs are opioid receptor-mediated. *Biochem Pharmacol* **195**, 114805 (2022).

99. Drug Enforcement Administration, D. of Justice. *Schedules of Controlled Substances: Placement of Furanyl Fentanyl, 4- Fluoroisobutyryl Fentanyl, Acryl Fentanyl, Tetrahydrofuranyl fentanyl, and Ocfentanil in Schedule I. Final order. Federal register.* (2018).
100. European Monitoring Centre for Drugs and Drug Addiction (EMCDDA). *Europol Joint Report on a new psychoactive substance: N-phenyl-N-[1-(2-phenylethyl)piperidin-4-yl]-furan-2-carboxamide (furanylfentanyl).* (2017).
101. Bilel, S. *et al.* In vitro and in vivo pharmaco-dynamic study of the novel fentanyl derivatives: Acrylfentanyl, Ocfentanil and Furanylfentanyl. *Neuropharmacology* **209**, 109020 (2022).
102. Fu, J., Jiao, J., Weng, K., Yu, D. & Li, R. Zebrafish methanol exposure causes patterning defects and suppressive cell proliferation in retina. *Am J Transl Res* **9**, 2975–2983 (2017).
103. Sant, K. E. & Timme-Laragy, A. R. Zebrafish as a Model for Toxicological Perturbation of Yolk and Nutrition in the Early Embryo. *Current environmental health reports* Preprint at <https://doi.org/10.1007/s40572-018-0183-2> (2018).
104. Varshneya, N. B. *et al.* Structurally diverse fentanyl analogs yield differential locomotor activities in mice. *Pharmacol Biochem Behav* **222**, 173496 (2023).
105. Sanchez-Simon, F. M. & Rodriguez, R. E. Developmental expression and distribution of opioid receptors in zebrafish. *Neuroscience* **151**, 129–137 (2008).
106. Gonzalez-Nunez, V. & Rodríguez, R. E. The zebrafish: A model to study the endogenous mechanisms of pain. *ILAR J* **50**, 373–386 (2009).
107. Ducharme, N. A., Reif, D. M., Gustafsson, J.-A. & Bondesson, M. Comparison of toxicity values across zebrafish early life stages and mammalian studies: Implications for chemical testing. *Reproductive Toxicology* **55**, 3–10 (2015).
108. Gaulier, J. *et al.* In vitro characterization of NPS metabolites produced by human liver microsomes and the HepaRG cell line using liquid chromatography-high resolution mass spectrometry (LC-HRMS) analysis: application to furanyl fentanyl. *Curr Pharm Biotechnol* (2017) doi:10.2174/1389201018666171122124401.
109. Watanabe, S. *et al.* In Vitro and In Vivo Metabolite Identification Studies for the New Synthetic Opioids Acetylfentanyl, Acrylfentanyl, Furanylfentanyl, and 4-Fluoro-Isobutyrylfentanyl. *AAPS Journal* (2017) doi:10.1208/s12248-017-0070-z.
110. Allibe, N. *et al.* Fatality involving ocfentanil documented by identification of metabolites. *Drug Test Anal* **10**, 995–1000 (2018).
111. European Monitoring Centre for Drugs and Drug Addiction (EMCDDA). *EU Early Warning System Formal Notification: 2-Methyl-AP-237.* (2019).
112. Krotulski, A. J., Fogarty, M. F. & Logan, B. K. AP-237. (2019).
113. Resnik, K., Brandão, P. & Alves, E. A. DARK Classics in Chemical Neuroscience: Bucinnazine. *ACS Chem Neurosci* **12**, 3527–3534 (2021).
114. Fogarty, M. F. *et al.* Toxicological and pharmacological characterization of novel cinnamylpiperazine synthetic opioids in humans and in vitro including 2-methyl AP-237 and AP-238. *Arch Toxicol* **96**, 1701–1710 (2022).

115. European Monitoring Centre for Drugs and Drug Addiction (EMCDDA). *EMCDDA initial report on the new psychoactive substance N,N-diethyl-2-[[4-(1-methylethoxy)phenyl]methyl]-5-nitro-1H-benzimidazole-1-ethanamine (isotonitazene)*. (2020) doi:10.1093/tandt/ttm111.
116. World Health Organisation. *Critical review report: isotonitazene*. (2020).
117. Hasegawa, K., Minakata, K., Suzuki, M. & Suzuki, O. Non-fentanyl-derived synthetic opioids emerging during recent years. *Forensic Toxicol* **40**, 234–243 (2022).
118. Blanckaert, P. *et al.* Report on a novel emerging class of highly potent benzimidazole NPS opioids: Chemical and in vitro functional characterization of isotonitazene. *Drug Test Anal* **12**, 422–430 (2020).
119. Walton, S. E., Krotulski, A. J. & Logan, B. K. A Forward-Thinking Approach to Addressing the New Synthetic Opioid 2-Benzylbenzimidazole Nitazene Analogs by Liquid Chromatography–Tandem Quadrupole Mass Spectrometry (LC–QQQ–MS). *J Anal Toxicol* **46**, 221–231 (2022).
120. Vandeputte, M. M. *et al.* Synthesis, Chemical Characterization, and μ -Opioid Receptor Activity Assessment of the Emerging Group of ‘nitazene’ 2-Benzylbenzimidazole Synthetic Opioids. *ACS Chem Neurosci* **12**, 1241–1251 (2021).
121. Grigoryev, A., Kavanagh, P., Dowling, G. & Rodin, I. Tentative Identification of Etazene (Etodesnitazene) Metabolites in Rat Serum and Urine by Gas Chromatography–Mass Spectrometry and Accurate Mass Liquid Chromatography–Mass Spectrometry. *J Anal Toxicol* **46**, 1032–1037 (2023).
122. Blanckaert, P. *et al.* Analytical characterization of “etonitazepyne,” a new pyrrolidinyll-containing 2-benzylbenzimidazole opioid sold online. *Drug Test Anal* **13**, 1627–1634 (2021).
123. Vandeputte, M. M. *et al.* Pharmacological evaluation and forensic case series of N-pyrrolidino etonitazene (etonitazepyne), a newly emerging 2-benzylbenzimidazole ‘nitazene’ synthetic opioid. *Arch Toxicol* **96**, 1845–1863 (2022).
124. Schumann, J. L. *et al.* Erratum: Intoxications in an Australian Emergency Department Involving “Nitazene” Benzylbenzimidazole Synthetic Opioids (Etodesnitazene, Butonitazene and Protonitazene) (Journal of Analytical Toxicology (2022) (bkac062) DOI: 10.1093/jat/bkac062). *J Anal Toxicol* **47**, E21 (2023).
125. Glatfelter, G. C. *et al.* Alkoxy chain length governs the potency of 2-benzylbenzimidazole ‘nitazene’ opioids associated with human overdose. *Psychopharmacology (Berl)* (2023) doi:10.1007/s00213-023-06451-2.
126. Drug Enforcement Administration, D. of Justice. *Benzimidazole-Opioids Other Name : Nitazenes*. https://www.deadiversion.usdoj.gov/drug_chem_info/benzimidazole-opioids.pdf (2022).
127. Baba, S. & Morishita, S.-I. Studies on Drug Metabolism by Use of Isotopes. XVI. Species Differences in Metabolism of 1-Butyryl-4-cinnamylpiperazine Hydrochloride. *Chemical Pharmaceutical Bulletin* **23**, 1949–1954 (1974).

128. Morishita, S.-I., Baba, S. & Nagase, Y. Studies on Drug Metabolism by Use of Isotopes XX: Ion Cluster Technique for Detection of Urinary Metabolites of 1-Butyryl-4-cinnamylpiperazine by Mass Chromatography. *J Pharm Sci* **67**, 757–761 (1978).
129. Hassanien, S. H., Layle, N. K., Holt, M. C. & Zhao, T. Generation of presumptive metabolites of a novel synthetic opioid using human liver microsomes and subsequent analysis by Orbitrap LC-MS/MS. *Poster presented at: Society of Forensic Toxicologists (SOFT) Annual Meeting 2019; October 13-18, 2019; San Antonio, TX.* (2019).
130. Krotulski, A. J., Papsun, D. M., Kacinko, S. L. & Logan, B. K. Isotonitazene Quantitation and Metabolite Discovery in Authentic Forensic Casework. *J Anal Toxicol* **44**, 521–530 (2021).
131. Krotulski, A. J., Papsun, D. M., Walton, S. E. & Logan, B. K. Metonitazene in the United States—Forensic toxicology assessment of a potent new synthetic opioid using liquid chromatography mass spectrometry. *Drug Test Anal* **13**, 1697–1711 (2021).
132. World Health Organisation. *Critical review report : Etazene (etodesnitazene).* (2022).
133. National Center for Biotechnology Information. PubChem Compound Summary for CID 156588955, Butonitazene. Retrieved April 13, 2023 <https://pubchem.ncbi.nlm.nih.gov/compound/Butonitazene>. (2023).
134. Papsun, D. M., Krotulski, A. J. & Logan, B. K. Proliferation of Novel Synthetic Opioids in Postmortem Investigations After Core-Structure Scheduling for Fentanyl-Related Substances. *American Journal of Forensic Medicine and Pathology* **43**, 315–327 (2022).